CrossMark

REVIEW

Polypyrrole composites with carbon materials for supercapacitors

Jingping Wang[1] · Xiao Li[1] · Xianfeng Du[2] · Jie Wang[2] · Hongrui Ma[1] ·
Xinli Jing[3]

Abstract Supercapacitors fill the gap between batteries and conventional solid state and electrolytic capacitors. Polypyrrole (PPy) is a very important electrode material for supercapacitors. However, the repeated volume changes usually damage PPy structure and result in PPy poor stability during a long-term charging/discharging process. PPy/carbon material composites were prepared to overcome the defects of pure PPy electrodes, and significant enhancement for the specific capacitance, charging/discharging rate and electrodes stability was demonstrated thereafter. The development of composite electrodes based on PPy and carbon materials is reviewed in this paper.

Keywords Supercapacitors · Polypyrrole · Carbon nanotube · Graphene · Carbon fiber · Carbon aerogel

Abbreviations

PPy	Polypyrrole
EDLCs	Electrical double-layer capacitors
ECs	Electrochemical pseudocapacitors
AC	Activated carbon
CNTs	Carbon nanotubes
CFs	Carbon fibers
CA	Carbon aerogels
GP	Graphene
PVS^{n-}	Polyvinylsulfonate
PSS^{n-}	Polystyrenesulfonate
DS^-	Dodecylsulfate
NS^-	1-Naphthalenesulfonate
COP	Chemical oxidation polymerization
EOP	Electrochemical oxidation polymerization
VA-CNTs	Vertically aligned CNTs
MWNTs	Multi-walled carbon nanotubes
CVD	Chemical vapor deposition
SWNTs	Single-walled carbon nanotubes
PPy/P-CNTs	Polypyrrole/plasma-activated CNTs
CTAB	Cetyltrimethylammonium bromide
CFP	Carbon fibers paper
PECVD	Chemical vapor deposition
EPD	Electrochemical pulse deposition
N-AC-MWNTs	Nitrogen-doped AC-coated MWCNTs
GO	Graphene oxide
RGO	Reduced graphene oxide
SG	Sulfonated graphene
MG/PPy	Macroporous graphene/polypyrrole
GP/PA	Graphene/polypyrrole aerogel
EPD	Electrophoretic deposition
FSSC	Fiber-shaped supercapacitors
PVA/H$_2$SO$_4$	Polyvinyl alcohol/H$_2$SO$_4$
NG/PPy	N-doped graphene/polypyrrole
PPy-NFs	Polypyrrole nanofibers
PPy-CNTs	Polypyrrole-coated carbon nanotubes
PPy/P(DMcT)/CFs	Polypyrrole/poly 2,5-dimercapto-1,3,4-thiadiazole/carbon fibers
N-CNFs	Nitrogen-doped carbon nanofibers
PPy/CCB	Polypyrrole/conductive carbon black

✉ Jingping Wang
   wangjingping@sust.edu.cn

✉ Xinli Jing
   xljing@xjtu.edu.cn

1 College of Chemistry and Chemical Engineering, Shaanxi University of Science and Technology, Xi'an 710021, China

2 Electronic Materials Research Laboratory, Key Laboratory of the Ministry of Education, Xi'an Jiaotong University, Xi'an 710049, China

3 Department of Applied Chemistry, School of Science, Xi'an Jiaotong University, Xi'an 710049, China

| GO/CNF | Graphene oxide/carbon nanofiber films |
| CNF/GP/PPy | Foam carbon nanofiber/graphene/ polypyrrole |

Induction

Supercapacitors (also called ultracapacitors) are usually used to describe an energy storage device which bridges the gap between batteries and dielectric capacitors (Simon and Gogotsi 2008; Winter and Brodd 2004). Recently, supercapacitors attract more and more attentions due to their features, including high power density, rapid charging/discharging rate, low cost and long cycling life (Jurewicz et al. 2001; Pandolfo and Hollenkamp 2006; Wang et al. 2012a; Winter and Brodd 2004). These features have aroused great interest in many fields, such as portable electronics, hybrid electric vehicles and wind power.

Generally, supercapacitors can be divided into two areas based on the mode of energy storage, namely electrical double-layer capacitors (EDLCs) and electrochemical pseudocapacitors (ECs) (Simon and Gogotsi 2008; Wang et al. 2012a).

EDLCs store energy based on the same mechanism as a traditional capacitor, i.e., charges at all electrode/electrolyte interfaces, as shown in Fig. 1. The double layer formation at EDLCs electrode interface has a time constant of $\sim 10^{-8}$ s, which is almost equal to that of its relaxation (Winter and Brodd 2004). Therefore, the double layer can respond rapidly when the potential changes. This interface storage way allows better power performance of EDLCs (Frackowiak, 2007; Winter and Brodd 2004). The charging/discharging process of EDLCs involves a charge

refabrication with extremely small volume change, not a chemical reaction (Arcila-Velez and Roberts 2014). This is main reason of high reversibility and good cycling stability (10^6 cycles). The electrode of EDLCs usually contains porous materials with high surface area, such as activated carbon (AC), carbon nanotubes (CNTs), carbon fibers (CFs), carbon aerogels (CA), and graphene (GP) (Frackowiak and Béguin 2001; Liu et al. 2010). Desired parameters for EDLCs electrode materials include high conductivity, tailorable morphology, large surface area with controlled pore structure, low cost, high purity, and low toxicity, excellent thermal stability, and reproducibility (Chandra et al. 2009; Singh and Chandra 2013). Most commercially available supercapacitors use carbon materials as electrode material, especially AC with large surface area and low cost (Frackowiak, 2007; Simon and Gogotsi 2008; Singh and Chandra 2013). However, the porous carbon materials fail to achieve high capacitance performance. The electrode materials with novel structure and correspondent electrolytes for EDLCs application should be well designed to further improve the capacitance performance in the future.
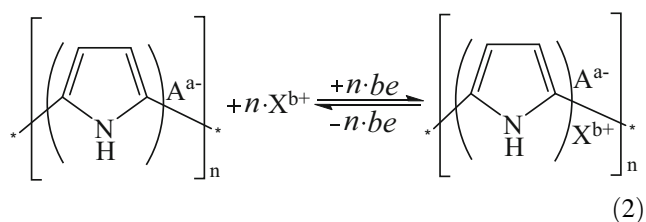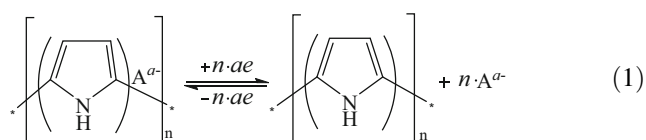
ECs store energy based on fast and reversible faradaic reactions in the bulk near the surface of electroactive materials (Lu et al. 2012a; Snook et al. 2011). In general, ECs store a greater amount of capacitance per gram than EDLCs, which meets the demand in various applications with high energy density and long operating time. Metal oxides (e.g., RuO_2, SnO_2, MnO_2 or Fe_3O_4, etc.) and electronically conducting polymers (e.g., polyaniline, PPy, polythiophene, etc.) have been extensively studied as ECs electrode materials in the past decades (De Adhikari et al. 2015; Simon and Gogotsi 2008; Wang and Zhang 2013). But due to redox reaction occurring which is closely related

Fig. 1 Charging/discharging process of electrical double-layer in symmetric supercapacitors

+Positive charge ⊕Cation ●Anion −Negative charge
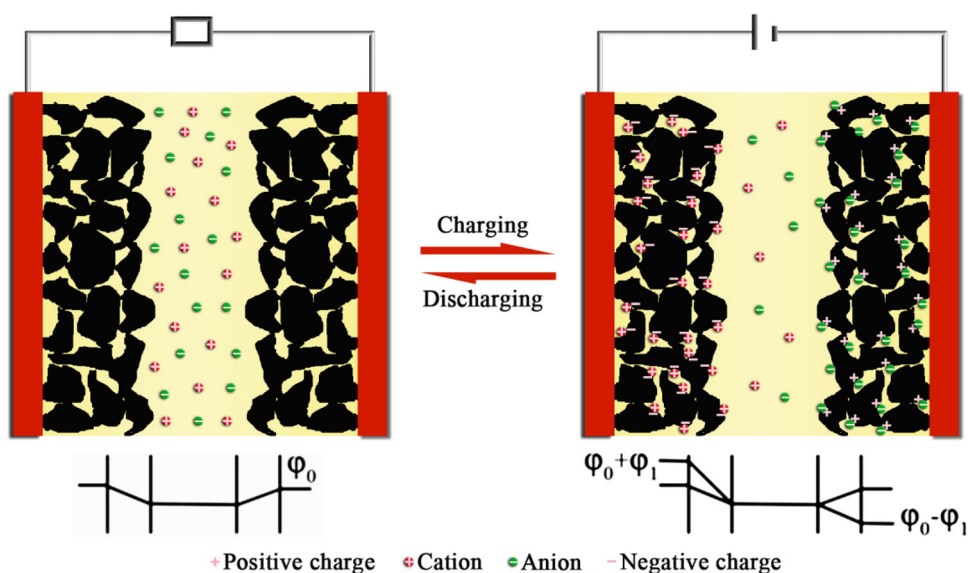
to various polarizations resulting from, for example, kinetic barriers for electron transfer, ohmic resistance and ion transport difficulty, ECs often suffer from the drawbacks of poor electronic conductivity and limited cycling life (Simon and Gogotsi 2008; Xu et al. 2014), which hinders the commercialization of many ECs electrode materials.

Polypyrrole (PPy) is one of most important electrode materials for ECs. PPy presents several advantages, such as easy synthesis, low cost, low toxicity, high electrical conductivity, good redox properties and environmental stability (Ata and Zhitomirsky 2015; Davies et al. 2011; Sadki et al. 2000). Snook et al. 2011 have given the typical differences between PPy and several other family forms (polyaniline and derivatives of polythiophene), which indicated that PPy has balanced electrochemical properties for ECs electrode. The mechanism of PPy energy storage can be described by Eq. 1 or Eq. 2 as shown below:

$$\left[\underset{\substack{H}}{\begin{array}{c} \\ N \end{array}} A^{a-} \right]_n \underset{-n \cdot ae}{\overset{+n \cdot ae}{\rightleftharpoons}} \left[\underset{\substack{H}}{\begin{array}{c} \\ N \end{array}} \right]_n + n \cdot A^{a-} \quad (1)$$

$$\left[\underset{\substack{H}}{\begin{array}{c} \\ N \end{array}} A^{a-} \right]_n + n \cdot X^{b+} \underset{-n \cdot be}{\overset{+n \cdot be}{\rightleftharpoons}} \left[\underset{\substack{H}}{\begin{array}{c} \\ N \end{array}} \underset{X^{b+}}{A^{a-}} \right]_n \quad (2)$$

where A^{a-} represents the dopant anions in PPy matrix, and X^{b+} for cations in working electrolyte. The charging/discharging process is performed mainly by the anions of A^- when the doped ions are the small ones, such as Cl^-, ClO_4^-, SO_4^- and NO_3^-. On the contrary, the charging/discharging process is performed mainly by the cations of X^+ when the doped ions is the large anions, such as polyvinylsulfonate (PVS^{n-}) and polystyrenesulfonate (PSS^{n-}), due to the immobility of these ions in the polymer matrix. In addition, the anions and cations largely involve the charging/discharging process when the doped ion is the bivalent anions or the anions with moderate size, such as dodecylsulfate (DS^-), 1-naphthalenesulfonate (NS^-) (Syritski et al. 2003; Weidlich et al. 2005). As is shown in Fig. 2, when PPy is used as both positive and negative electrodes, PPy volume and doped level change greatly in charging/discharging process.

Methods for PPy synthesis include chemical polymerization by chemical oxidants and electropolymerization by anodic oxidation. PPy powder with high surface area can be easily achieved via chemical oxidation polymerization

(COP). Concerning PPy powder application in supercapacitors, most electrodes are porous structures in which an interconnected matrix composed of PPy particles, a polymer binder to hold the mix together and bond the mix to a conductive current collector, and other component, are filled with electrolyte (Winter and Brodd 2004). Typically, polymer binder on PPy particle surface hinders the transportation of ions and electrons and increases the internal resistance of supercapacitors. So the addition of a conductive component to simultaneously improve electronic and ions transport in composite electrode has been a research focus of PPy supercapacitors (Chen et al. 2012; Dubal et al. 2012; Yang et al. 2015a; Zhang et al. 2013).

PPy active material prepared by electrochemical oxidation polymerization (EOP) is an electroactive film attached to the substrate electrode. Most PPy films via electropolymerization have high electrical conductivity and typical "cauliflower" structure that is often dense (Wang et al. 2010). It is obvious that dense structure can block ions diffusion from film surface to film internal layer. In other word, the specific capacitance of PPy electrode decreases when PPy film became thicker (Wang et al. 2012b). In fact, the charge storage behavior of pseudocapacitive materials is strongly dependent on the mass loading in practical energy storage devices. Thus, the mass loading of conventional electrodes increases nothing but "dead" materials, the part of which is not accessible to electrolyte (Cai et al. 2015a). At present, the critical question for electropolymerized PPy films is how to improve the porosity of PPy films and increase utilization efficiency of the active materials while their electrical conductivity do not decrease too much simultaneously.

In any case, the insertion/extrusion of ions from PPy matrix has to result in big volume change, especially at a wide potential window (Otero et al. 1997), as shown in Fig. 2. The repeated big volume change usually damage PPy structure (Wang et al. 2011). At the same time, the overoxidation at PPy backbone and the formation of the compensating semiconductor state in PPy matrix can induce the decay of PPy electrochemical performance (Debiemme-Chouvy and Tran 2008; Marchesi et al. 2011; Wang et al. 2011, 2014a). Noting that the big volume change usually weaken the bond between the current collector and PPy active material because the volume of current collector does not change simultaneously during PPy charging/discharging process, which has to increase the internal resistance of supercapacitors. These can become the main reason of the limited cycling life of PPy at different operating conditions. Therefore, many researches focused on what causing decline of PPy stability during long-term charging/discharging process (Liang et al. 2014; Lim et al. 2014; Raj et al. 2015; Snook et al. 2011).

Fig. 2 Charging/discharge process of PPy in symmetric supercapacitors
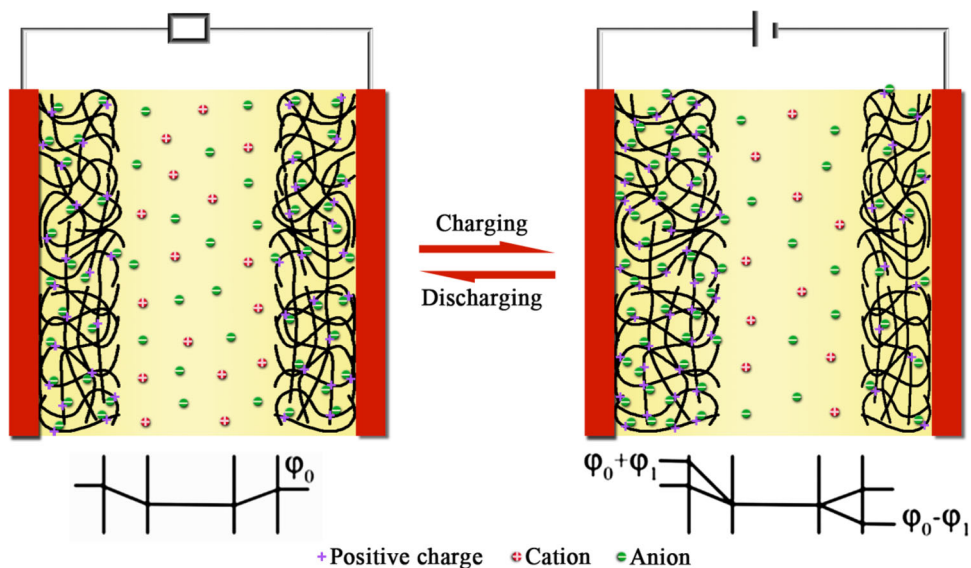
Many methods have been implemented to overcome the defects of PPy electrodes (Raudsepp et al. 2008; Sharma et al. 2008; Wang et al. 2010; 2014a Zhu and Zhitomirsky 2013). Preparation of PPy composites is one of the most common methods to improve its capacitance properties for supercapacitors (Aradilla et al. 2015; Simon and Gogotsi 2008; Snook et al. 2011). Several researchers have given some suggestions from different aspects in their review papers (Nyholm et al. 2011; Simon and Gogotsi 2008; Snook et al. 2011; Wang et al. 2012b). However, with rapid development of carbon materials in recent years, great attentions were paid to PPy composites with various carbon materials, such as CNTs, GP, CFs, AC, CA, glassy carbon, etc, and the several key characteristics of PPy electrodes were improved obviously (Frackowiak 2007; Liu et al. 2010; Meyyappan 2013; Simon and Gogotsi 2008; Wang et al. 2009; Wu and Lin 2006). Thus, this review will focus on the composites of PPy with various carbon materials.

PPy/CNTs composites for supercapacitors

Since the first report on quasi-one-dimensional CNTs by Ijima in 1991, investigations on their growth, characterization and application have grown exponentially due to their high conductivity, excellent mechanical performance, large specific area and various forms available, such as vertically aligned CNTs (VA-CNTs) film, planar film with random or aligned networks of CNTs, transparent film, stretchable nonwoven cloth and compressible foams (Cai et al. 2015a; Hussain et al. 2015; Li et al. 2014; Raymundo-Pinero et al. 2011; Treacy et al. 1996; Wu et al. 2004). Quantum mechanics calculations predict that defect-free single-walled carbon nanotubes possess Young's modulus

values of ~ 1 Tpa, tensile strengths >100 Gpa (Peng et al. 2008; Treacy et al. 1996). The thermal conductivity of MWCNTs exceeds 3000 W/(m K), which is about twice as high as diamond (Kim et al. 2001). In multi-walled carbon nanotubes (MWNTs) matrix, extremely high stable current densities, $J > 10^7$ amperes per square centimeter, have been attained without being destroyed (Frank et al. 1998). In addition, CNTs can be easily prepared by three methods, namely arc discharge, laser ablation, and chemical vapor deposition (CVD) (Hussain et al. 2015). The basic elements for the formation of nanotubes contain only catalyst, a source of carbon, and sufficient energy. Due to their exceptional combination of mechanical, thermal, chemical, and electronic properties, single-walled carbon nanotubes (SWNTs) and MWNTs are considered as unique materials, with very promising future applications, especially in the field of nanotechnology, nanoelectronics, and composite materials (Kharisov et al. 2009).

The extraordinary properties mentioned above about CNTs render them as the ideal candidates for PPy reinforcing in charging/discharging process. The PPy/CNTs composites are often prepared by several methods, namely EOP, COP and electrophoretic deposition (Khomenko et al. 2005; Su and Zhitomirsky 2015). The COP of PPy is suitable to mass production of the materials, though PPy on CNTs usually supplies a nonhomogeneous type of deposit with a tendency to form some aggregates. The EOP of PPy/CNTs composites are limited in terms of mass production of the materials, and also it is not suitable for preparing composites with a large proportion of polymer (Khomenko et al. 2005). Nevertheless, the EOP gives a very unique deposit of a homogeneous PPy film which exhibits a good conductivity and provides a better control of PPy thickness and morphology on CNTs surface (Jurewicz et al. 2001). In

Table 1 Description of PPy/CNT composites

Synthesis method	Capacitance	Stability	References
COP	163 F g^{-1} (0.17 A g^{-1})		Jurewicz et al. (2001)
COP	192 F g^{-1} (5 mV s^{-1})	92% (Asy., 100 cycles, 0.6 V)	Khomenko et al. (2005)
COP	200 F g^{-1} (200 mV s^{-1})		Wang et al. (2007)
COP	167.2 F g^{-1} (0.5 mA cm^{-2})	>95% (500 cycles, 0.6 V, 0.5 mA cm^{-2})	Paul et al. (2010)
COP	152.78 F g^{-1} (0.32 A g^{-1})	85% (5000 cycles, 2 V, 0.32 A g^{-1})	Lee et al. (2011)
COP	357 F g^{-1} (0.25 A g^{-1})	>97% (1000 cycles, 1.3 V, 1 A g^{-1})	Fu et al. (2011)
COP	165 F g^{-1} (0.5 mA cm^{-2})	100% (1000 cycles, 0.6 V, 0.5 mA cm^{-2})	Paul et al. (2012)
COP	124 F g^{-1} (0.19 A g^{-1})	94% (Asy., 1000 cycles, 1.05 V, 200 mV s^{-1})	Zhou et al. (2012)
COP	228 F g^{-1} (0.5 A g^{-1})		Han et al. (2012)
COP	4.1 F cm^{-2} (2 mV s^{-1})	94% (1000 cycles, 0.9 V, 50 mV s^{-1})	Shi and Zhitomirsky (2013b)
COP	4.62 F cm^{-2} (2 mV s^{-1})	104.2% (1000 cycles, 0.9 V, 50 mV s^{-1})	Shi and Zhitomirsky (2013c)
COP	183.2 F g^{-1} (8 A g^{-1})	94.2% (1000 cycles, 1 V, 1 A g^{-1})	Fu et al. (2013)
COP	262 F g^{-1} (0.4 A g^{-1})	96.3% (450 cycles, 1 V, 20 mV s^{-1})	Liu et al. (2014)
COP	376 F·g^{-1} (0.5 A·g^{-1})	>90% (1000 cycles, 0.45 V, 20 mV s^{-1})	Li et al. (2014)
COP	264.8 F·g^{-1} (2 mV·s^{-1})	94.2% (5000 cycles, 1 V, 1.11 A g^{-1})	Zhu et al. (2014a)
COP	179 F g^{-1} (2 mV s^{-1})	84.3% (Asy., 1000 cycles, 1.3 V, 0.2 A g^{-1})	Su and Zhitomirsky (2015)
COP	4.2 F cm^{-2} (2 mV s^{-1})	101% (5000 cycles, 0.9 V, 50 mV s^{-1})	Zhu et al. (2014b)
COP	56 F g^{-1}, 202 mF cm^{-1} (0.2 A g^{-1})	100% (2000 cycles, 0.8 V, 1 A g^{-1})	Xu et al. (2015a)
COP	264 F g^{-1} (10 mV s^{-1})	89% (1000 cycles, 0.7 V, 5 mA cm^{-2})	Yang et al. (2015a)
EOP	890 F g^{-1} (2 mV s^{-1})	91% (1000 cycles, 0.5 V, 20 mV s^{-1})	Lin and Xu (2008)
EOP	250 F g^{-1} (10 mV s^{-1})		Kim et al. (2008)
EOP	310 F g^{-1} (2 mV s^{-1})	85% (1000 cycles, 0.9 V, 50 mV s^{-1})	Shi and Zhitomirsky (2011)
EOP	264.8 F g^{-1} (2 mV s^{-1})		Li et al. (2012)
EOP	240 F g^{-1} (10 mV s^{-1})	93.49% (1000 cycles, 0.6 V, 1 A g^{-1})	Sun et al. (2012)
EOP	390 F g^{-1} (2 mV s^{-1})		Li and Zhitomirsky (2013)
EOP	274 F g^{-1} (2 mV s^{-1})		Chen and Zhitomirsky (2013)
EOP	472 F g^{-1} (5 mV s^{-1})	89.9% (1000 cycles, 0.6 V, 0.2 A g^{-1})	Zhang et al. (2013)
EOP	4.9 F cm^{-3} (0.05 A cm^{-3})	95% (10,000 cycles, 0.8 V, 0.1 A cm^{-3})	Chen et al. (2015b)

Capacitance—specific capacitance (charging/discharging rate), stability—retained capacitance (cycle number, voltage window, charging/discharging rate)

available research results, most of PPy/CNTs composites were prepared by COP method, which is shown in Table 1. The earlier researches were generally based on COP method (Fan et al. 1999a, b; Jurewicz et al. 2001; Khomenko et al. 2005; Xiao and Zhou 2003).

CNTs dispersion

CNTs functionalization

The dispersion of CNTs is very important to improve the electrochemical performance of PPy/CNTs composites because most of CNTs cannot enter composite matrix when an uneven dispersion occurs in polymerization electrolyte. It was found that the treatment of CNTs by acids or air plasma showed improved dispersion and can be used for the fabrication of PPy/CNTs composites (Han et al. 2012; Hussain et al. 2015; Kharisov et al. 2009; Sun et al. 2012;

Tasis et al. 2006; Wang et al. 2007; Yang et al. 2015a; Zhang et al. 2013). A suitable functionalization time in acids is the key for preparing PPy/CNTs composites because too long time can result in more defects on the CNT sidewalls (Sun et al. 2012). After SWNTs were functionalized and cut for 48 h in a concentrated H_2SO_4/HNO_3 solution, the PPy/acids-functionalized SWNTs composites were prepared and showed the specific capacitance of 200 F g^{-1} at a scanning rate of 200 mV s^{-1} (or >0.6 Fcm^{-2}) (Jie Wang et al. 2007). The PPy/plasma-activated CNTs composites (PPy/P-CNTs) were prepared via a chemical oxidation polymerization (Yang et al. 2015a). The results indicated that not only the interaction of the π bond on the CNT and PPy but also the oxygen-containing and nitrogen-containing groups via air plasma activation on the surface of the P-CNTs played important role in the tightly coating PPy on the P-CNTs. The specific capacitance of PPy/P-CNTs composites reached 264 F g^{-1}

in 1 M H_2SO_4 at a CV scan rate of 10 mV s^{-1} and retained approximately 89% of its initial capacitance after 1000 charge–discharge cycles at a current density of 5 mA cm^{-2}.

CNTs dispersion with surfactants

However, the functionalization process that creates active groups has to induce defects on the CNT sidewalls and reduce the electronic conductivity and mechanical property of CNTs (Zhu et al. 2014a). Therefore, the CNTs functionalization should be avoided if other ways can adequately improve the CNTs dispersion. Physical approaches using amphiphilic surfactants have been demonstrated to be capable of debundling SWNTs and stabilizing individual tubes while maintaining CNTs integrity and intrinsic properties (Kharisov et al. 2009; Tasis et al. 2006; Wang 2009; Wu et al. 2004). Surfactants disperse CNTs in aqueous solutions basing on hydrophobic/hydrophilic interactions, in which the hydrophobic tail of the surfactant molecule adsorbs on the surface of CNTs bundles while the hydrophilic head associates with water for dissolution. Figure 3 shows some surfactants used to disperse CNTs in different solvents (Chen and Zhitomirsky 2013, 2014; Fu et al. 2013; Li et al. 2012; Li and Zhitomirsky 2013; Shi and Zhitomirsky 2011; Shi and Zhitomirsky 2015a; Shi et al. 2014; Shi and Zhitomirsky 2013b, 2013c, 2015, 2015b; Wu and Lin 2006; Yang et al. 2015c; Zhu et al. 2014a, b). Zhitomirsky group has made a lot of researches on dispersing CNTs by surfactants for preparing PPy/CNTs composites (Chen and Zhitomirsky 2013,2014; Li et al. 2012; Li and Zhitomirsky 2013; Shi and Zhitomirsky 2011, 2013b, 2013c, 2015b, 2015 Shi et al. 2014; Yang et al. 2015c; Zhu et al. 2014a, b). Cetyltrimethylammonium bromide (CTAB) is one of the most common surfactants for PPy/CNTs preparation. When CTAB was used as a soft template to prepare PPy/CNTs composites, which showed a specific capacitance of 183.2 F g^{-1} at a current density of 8 A g^{-1} (Fu et al. 2013). The specific capacitance retention was 85% after 1000 cycles at 1 A g^{-1}. At the same time, the asymmetric supercapacitors fabricated using PPy/CNTs composites as a positive electrode and active carbon as a negative electrode displayed a capacitance retention of 72% at a current density of 1 A g^{-1} even after 3000 cycles.

The coverage of surfactant on CNTs surfaces essentially depends on the strength of attractive interactions. A comprehensive study of the interaction between modified atomic force microscopy tips and CNTs bucky paper based on experiments and simulations indicated that aryl-thiols endgroups have a more strong attraction to SWNTs than other endgroups (Wang 2009). The aromatic rings on surfactant molecules promoted their adsorption on CNTs due to the π–π interactions, whereas the charged groups of the adsorbed molecules provided electrostatic repulsion and dispersion of CNTs (Gupta et al. 2013). On the other hand, the surfactants with aryl-thiols can act as anionic dopants for PPy polymerization, which can promote the formation of uniform coatings and improve the adhesion strength between PPy films and CNTs surface (Zhu et al. 2014a). When the surfactants with aryl-thiols were used to disperse CNTs in the process of PPy/CNTs preparation, the capacitance and stability of PPy/CNTs composites were enhanced obviously in the work of Zhitomirsky group (Shi et al. 2014), as shown in Table 1.

Porous PPy/CNTs composites

High active material loading on the electrode is important to the practical application of supercapacitors. The simply increase of active material loading often results in an increase in "dead" materials and only increase internal resistance and decrease the specific capacitance of active material because the ions cannot insert the internal bulk of active material. At the same time, thick PPy films often show big capacitance degradation at high charging/discharging rate (Shi and Zhitomirsky 2013c). The porous structure with a high surface area usually facilitates solvent uptake and dopant ion access. However, the high surface areas did not always result in higher specific capacitances because the electrolyte cannot enter into the pores with very small pore diameter, indicating that the porosity of the active material should be optimized (Borchardt et al. 2014; Nyholm et al. 2011). Several strategies including the use of sacrificial template, the fabrication of 3D porous network matrix using VA-CNTs and CNTs sponge were used to obtain the porous PPy/CNTs composites (Cai et al. 2015a; Fang et al. 2010; Kim et al. 2008; Li et al. 2014; Warren et al. 2015; Zhang et al. 2013).

As shown in Fig. 4, a CNTs film electrode containing nano-size SiO_2 was fabricated using an electrostatic spray deposition and PPy was electrodeposited on to the CNTs (Kim et al. 2008). Then the nano-size SiO_2 was removed leaving a three-dimensional entangled structure of a PPy/CNTs film. The control of the pore size of composites film was performed by changing the amount of nano-silica in the mixed suspension for electrostatic spray deposition. The specific capacitance of a CNT/PPy composite with 83.4 wt.% PPy reached 250 F g^{-1} at a CV scan rate 10 mV s^{-1} in 1 M KCl and only decreased to 211 F g^{-1} while the CV scan rate increasing to 500 mV s^{-1}, which indicted that a high ions transport was obtain in CNT/PPy composites. In addition, the three-dimensional ordered macroporous (3DOM) PPy/CNTs composites were prepared through cyclic voltammetry copolymerization from a solution containing both acid-treated CNTs and pyrrole monomers while the SiO_2 colloidal crystal was used as the

Fig. 3 Chemical structures of common surfactants used to disperse SWNTs for preparing PPy/CNTs composites, (1) from Shi and Zhitomirsky (2013c), (2), (3) and (4) from Zhu et al. (2014a) (5) and (6) from Li and Zhitomirsky (2013), (7) from Fu et al. (2013), (8) from Shi and Zhitomirsky (2011), (9) from Chen and Zhitomirsky (2014), (10) and (16) from Shi and Zhitomirsky (2013b), (11) and (17) from Chen and Zhitomirsky (2013), (12) and (15) from Li et al. (2012), (13) and (14) from Su and Zhitomirsky (2015), (18) from Zhu et al. (2014b), (19) from Shi et al. (2015)
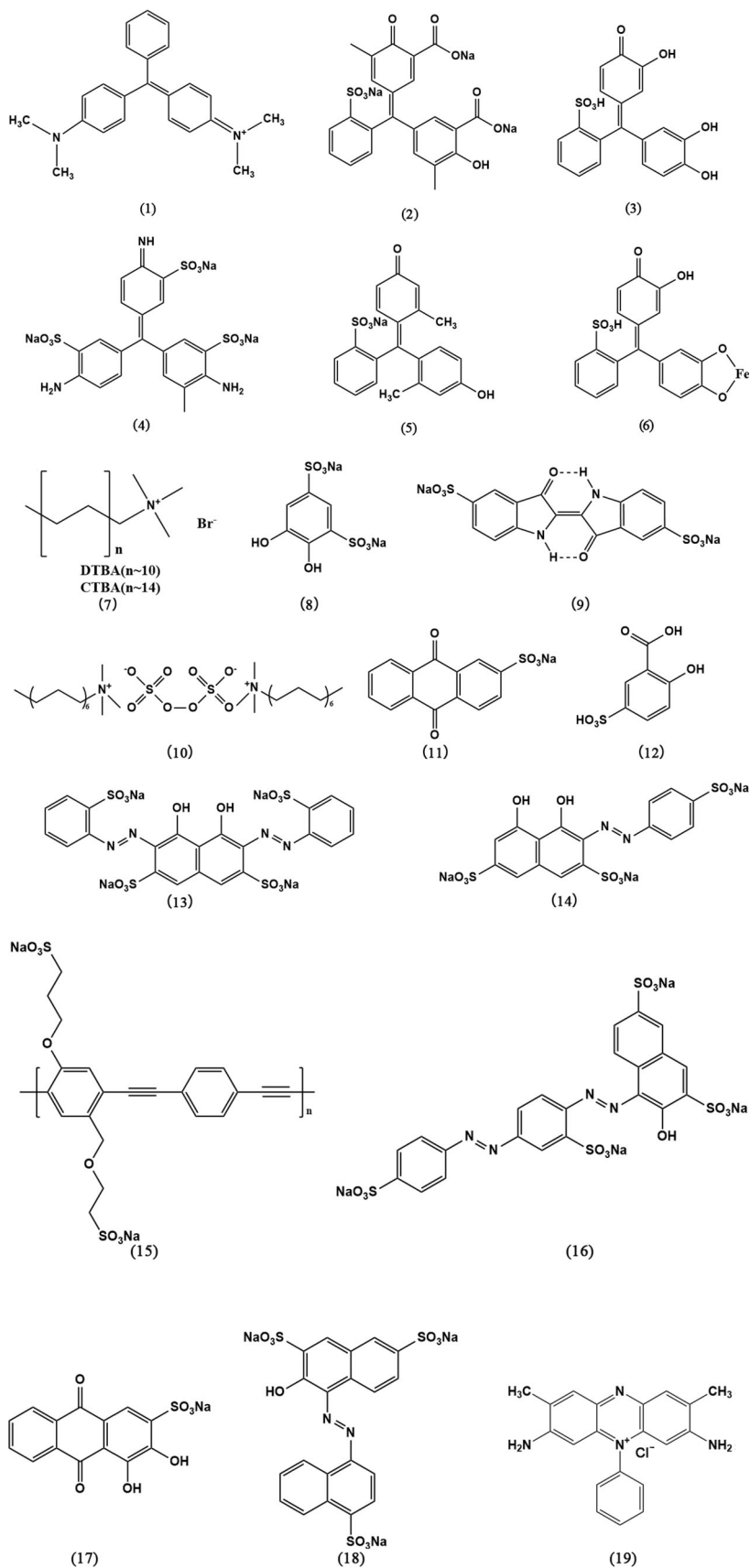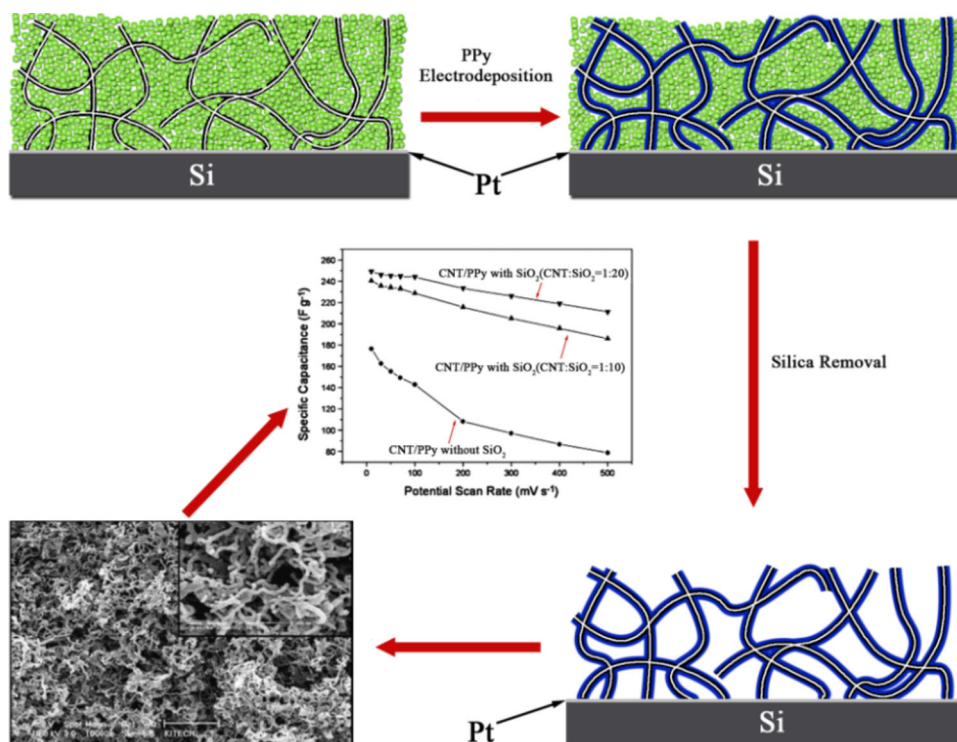
sacrificial template (Zhang et al. 2013). The specific capacitance of 3DOM PPy/CNTs composites reached 427 F g^{-1} at a CV scanning rate of 5 mV s^{-1}. In analysis modeling of Trasatti et al, the overall capacitance of a pseudocapacitive material was assumed to contain two contributions, Q_{out} and Q_{inn} (Baronetto et al. 1994). The Q_{inn} of the 3DOM CNT/PPy composite was 154.72 F g^{-1}, which is much larger than that of the planar film, proving that ion diffusion in 3DOM matrix contributed a lot to the charge storage. The 3DOM films also can provide ion flux with high migration rate, which can enhance the power output capability of supercapacitors.

Recently, the VA-CNTs with high aspect ratios that are arranged perpendicular to a substrate were used to prepare PPy/VA-CNTs composites due to its high specific surface area, low contact resistance to the metal electrode, high conductivity, controllable distance between the single nanotubes and length of nanotubes, as shown in Fig. 5 (Borchardt et al. 2014; Cai et al. 2015a; Warren et al. 2015). According to Cai et al, the VA-CNTs array on 3D CFs paper (CFP) were constructed by plasma-enhanced chemical vapor deposition (PECVD) system, and then PPy/VA-CNTs/CFP composites were prepared using COP method (Cai et al. 2015a). The specific capacitance values of PPy/VA-CNTs/CFP composites calculated from CVs reached 681, 568, 512, 480, and 384 F g^{-1} at CV scan rates of 2, 5, 10, 20 and 50 mV s^{-1}, respectively, corresponding to the areal capacitance of 0.78, 0.65, 0.58, 0.52 and 0.43 F cm^{-2}. The PPy/VA-CNTs/CFP composites retained 72% of its initial capacitance after 10,000

cycles. The capacitance retention can be related to the high loading of PPy/VA-CNTs/CFP composites. As shown in Fig. 5, the PPy/VA-CNTs composites can be obtained via EOP method (Warren et al. 2015). The specific capacitance of PPy/VA-CNTs composites reached 5 mF cm^{-2}, which is 500% higher than that of as-grown VACNT or pure PPy film. The enhanced energy storage should be attributed primarily to fast surface redox reaction on PPy.

The 3D CNTs sponge with a highly porous network structure was fabricated using chemical vapor deposition, and then was used as a substrate to prepare PPy/CNTs core–shell sponge by EOP method (Li et al. 2014). The PPy coating not only enhanced specific capacitance of the CNTs sponge to above 300 F/g but also reinforced the porous structure to achieve better strength and rebound elasticity. Noting that the appropriate PPy loading are a very important factor for the improvement of specific capacitance because the pores in composites matrix are easy to reduce and disappear when PPy thickness increase continuously. Thus, the thickness of PPy coating in different preparation process should be optimized (Fang et al. 2010; Li et al. 2014). In the work of (Fang et al. 2010), the electrochemical pulse deposition (EPD) was used to control the formation of PPy coating. The EPD method allows monomers to diffuse from the bulk solution into 3D matrix space between CNTs which should be very favorable to on CNTs surface. A high specific capacitance of 427 F g^{-1} in PPy/CNTs matrix has been achieved using EPD method.

Fig. 5 Fabrication process of PPy/VA-CNTs supercapacitor electrode
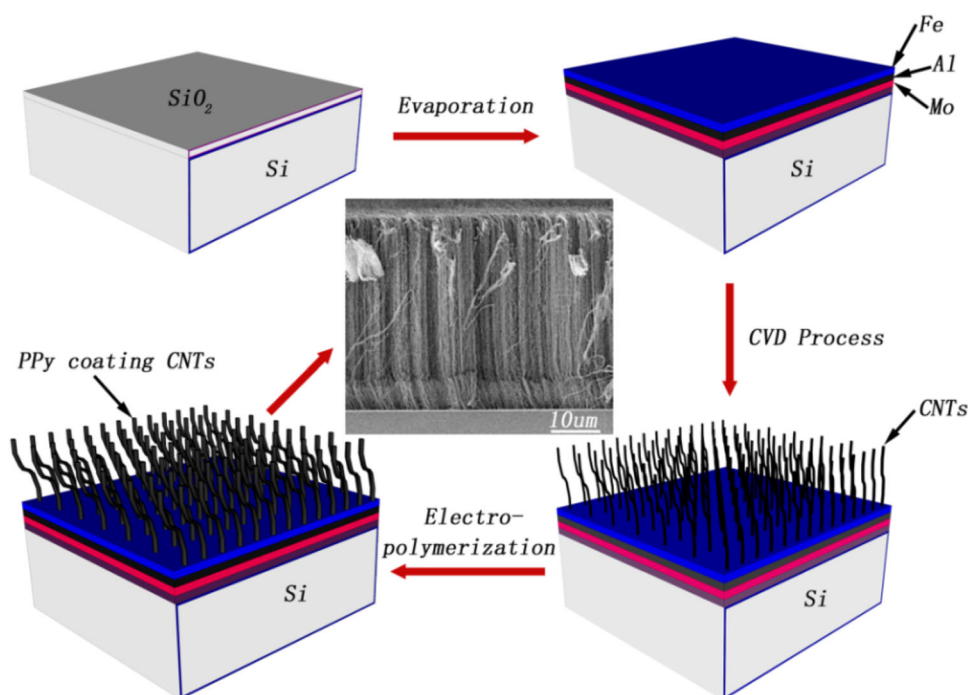
Application of PPy/CNTs composites in flexible supercapacitors

The rapid development of energy storage devices for wearable electronics requires designing the new versatile and flexible electrode materials as alternatives to batteries and supercapacitors (Kim et al. 2015; Nyholm et al. 2011; Tao et al. 2013). PPy/CNTs properties meet the most demands of flexible electrode materials, such as low cost, good flexibility, light weight and reliable environmental friendliness. As shown in Fig. 6, Py was deposited on as-prepared CNT films at a potential of 0.7 V (vs. SCE) and formed a core–shell PPy/CNTs nanocomposite (Xu et al. 2015a). After washing in deionized water, the nanocomposite strips were spun for about 10,000 turns per meter into fibers. The PPy/CNTs fibers exhibited a high specific capacitance of 350 F g^{-1} at 1 A g^{-1} in 1 M H_2SO_4 aqueous electrolyte. Furthermore, all-solid-state fiber-shaped supercapacitors (FSSC) with core–shell PPy/CNTs electrodes were fabricated using polyvinyl alcohol/H_2SO_4 (PVA/H_2SO_4) gel electrolyte. The specific capacitance of the CNTs-PPy FSSC reached 36 F g^{-1} (127 mF cm^{-1}, 588 mF cm^{-2}, 17 F cm^{-3}), which is seven times higher than that of the pure CNTs FSSC. While adding hydroquinone to gel electrolyte, the specific capacitance reached 56 F g^{-1} (202 mF cm^{-1}, 1168 mF cm^{-2}, 42 F cm^{-3}). The all-solid-state FSSCs showed high stability after 2000 cycles and good flexibility under bending, knotting, and suffering tension. Moreover, a very simply method was used to prepare PPy/CNT composites, i.e., the flexible
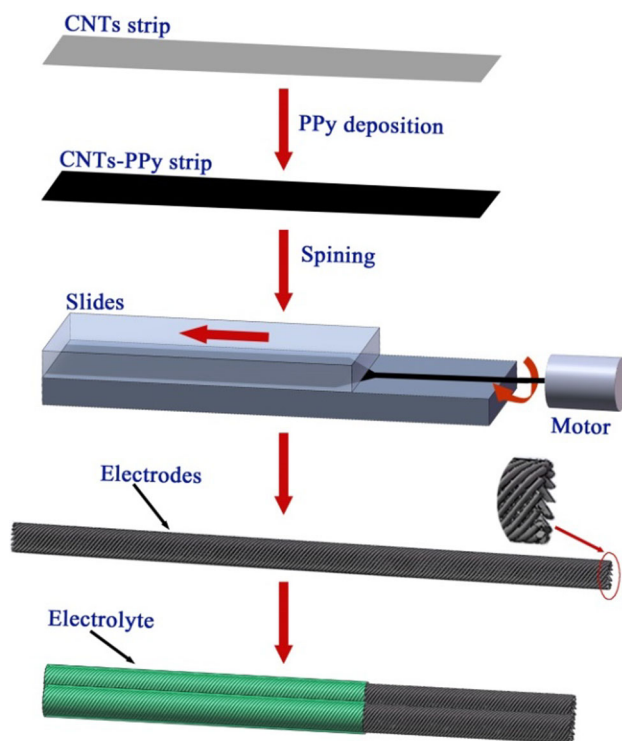

Fig. 6 Schematic of the fabrication process of all-solid-state fiber-shaped supercapacitors

CNTs film was fabricated by the vacuum filtration and used as substrate electrode for PPy electrochemical deposition (Chen et al. 2015b). The two pieces of PPy-coated CNTs composites were used as the electrodes for the flexible all-solid-state supercapacitors with a gel electrolyte of PVA/

H_2SO_4. The volumetric capacitance of the all-solid-state supercapacitors was calculated to be 4.9 F cm^{-3} at 0.05 A cm^{-3} and still remained 3 F cm^{-3} at 0.5 A cm^{-3}. The capacitance retention is larger than 95% after 10,000 cycles at a current density of 0.1 A cm^{-3}. The CV curves of the PPy-coated CNTs composites only exhibited slight changes when being bent or twisted, confirming the promising performance of flexible energy storage.

Nitrogen-doped CTNs from PPy/CNTs composites

The use of CTNs as an electrode material for supercapacitors offers the advantages of high electronic conductivity and good capacitance retention at high charging/discharging rates. However, the specific capacitance of CNTs is lower than that of activated carbon because of a low specific surface area of CNTs. Nitrogen-doped AC-coated MWCNTs (N-AC-MWNTs) exhibited good electrochemical performance while being used as supercapacitor electrodes (An et al. 2013; Shi et al. 2014; Shi and Zhitomirsky 2015a). As the precursor to N-AC-MWNTs (Shi et al. 2014), PPy/MWNT composites were fabricated using oxidant-surfactant nanocrystals. The N-AC-MWNTs composites were obtained by heating PPy/MWNT composites for carbonization in a tubular furnace under a nitrogen atmosphere at 700 °C for 2 h. The preparation process of N-AC-MWNTs composites was shown in Fig. 7. The N-AC-MWNTs electrodes showed the maximum specific capacitance of 103 F g^{-1} for the mass loading of 35 mg cm^{-2} at a scan rate of 2 mV s^{-1}. The aqueous supercapacitor cells based on N-AC-MWNTs electrodes exhibited the energy density of 16.1 mWh g^{-1} while its power density was 14.4 W g^{-1}. The N-AC-MWNTs electrodes retained 98.0% of its initial capacitance at a CV scan rate of 100 mV s^{-1} in the voltage window of 1.8 V after 1000 cycles. It is generally considered that N-doped carbon has not only introduce pseudocapacitance but also improve the wettability of carbons for electrolyte accessibility (An et al. 2013). Meanwhile, suitable pore texture possibly produced by the release of non-carbon elements or the burn of a small amount of carbon during the carbonization favors to form electric double-layer capacitance and ions transportation.

PPy/graphene composites for supercapacitors

Since the isolation of two-dimensional (2D) GP in 2004, it has rapidly grown up to be a superstar in the field of energy storage due to its exciting properties, such as a large theoretical specific surface area (2630 m^2 g^{-1}), high intrinsic mobility (200,000 cm^2 v^{-1} s^{-1}), high Young's modulus ($\sim$1.0 Tpa), high electrical conductivity, and good thermal conductivity ($\sim$5000 W m^{-1} K^{-1}) (Brownson et al. 2011; Zhu et al. 2010). GP as a supercapacitors material has been widely reported by many literatures, in which GP was described as a far superior supercapacitors material than existing carbon and polymer-based materials (Brownson et al. 2011; Kim et al. 2015; Wang et al. 2009). However, the specific capacitance of GP is not as high as expected due to the restacking of nanosheets driven by van der Waals interactions, and thus many researchers have turned to fabricate GP based hybrid materials for improving capacitance performance (Kim et al. 2015). Recently, the PPy/GP composites were fabricated via various methods. The coating on GP surface restrains the restacking of GP nanosheets and results in an unordered sheet structure with porous structure, which enhances the surface area of composites and provides the channels of ions diffusion. Therefore, PPy/GP composites as supercapacitors electrode often show high specific capacitance and charging/discharging rate. Moreover, the GP in PPy/GP matrix can act as reinforcing material for improving the stability of PPy electrode. On the other hand, GP does not often exhibit its anticipated performance in PPy/GP composites for supercapacitors, which should be related to the porous structure, the restacking of GP, the interface between PPy and GP. Table 2 shows the electrochemical performances of various PPy/GP composites.

Graphene dispersion

"Graphene" is often on behalf of several material, namely pristine GP, graphene oxide (GO), and reduced graphene oxide (RGO) (Johnson et al. 2015). In the available reports, GP in PPy/GP composites include two forms, i.e., GO and RGO. The hydrophilic or hydrophobic groups on GO and
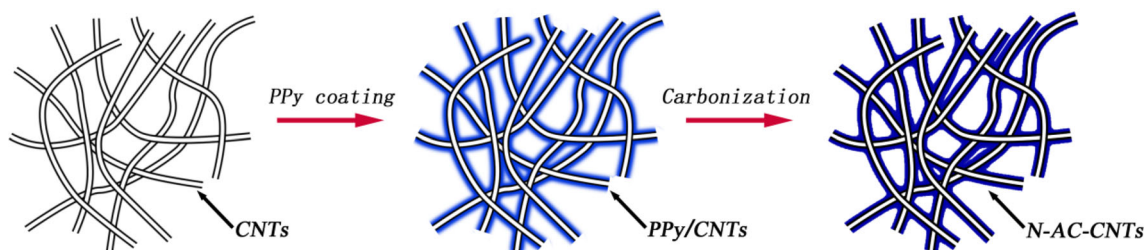

Fig. 7 Schematic illustration of the synthesis of N-AC-MWNTs

Table 2 Description of PPy/GP composites

Synthesis method	Capacitance	Stability	References
COP	165 F g^{-1} (1 A g^{-1})	92% (1000 cycles, 1 V, 1 A g^{-1})	Biswas and Drzal (2010)
COP	528 F g^{-1} (0.3 A g^{-1})	70% (1000 cycles, 0.8 V, 5 A g^{-1})	Zhang et al. (2010)
COP	1510 F g^{-1} (10 mV s^{-1})		Mini et al. (2011)
COP	394 F g^{-1} (2 mV s^{-1})	90% (540 cycles, 1 V, 0.26 A g^{-1})	Lai et al. (2012)
COP	400 F g^{-1} (0.3 A g^{-1})	88% (200 cycles, 1 V, 1.5 A g^{-1})	Liu et al. (2012)
COP	492 F g^{-1} (0.2 A g^{-1})	84% (1000 cycles, 1 V, 2 A g^{-1})	Mao et al. (2012)
COP	248 F g^{-1} (0.3 A g^{-1})	81% (1000 cycles, 1 V, 0.3 A g^{-1})	Zhang and Zhao (2012)
COP	728 F g^{-1} (0.5 A g^{-1})	93% (1000 cycles, 1 V, 50 mV s^{-1})	Li et al. (2013)
COP	261 F g^{-1} (1 A g^{-1})	87% (1000 cycles, 1 V, 50 mV s^{-1})	Wang et al. (2013)
COP	350 F g^{-1} (1.5 A g^{-1})	100% (1000 cycles, 50% compressive strain)	Zhao et al. (2013)
COP	360 F g^{-1} (1 A g^{-1})	72% (500 cycles, 1 V, 1 A g^{-1})	Bora and Dolui (2014)
COP	333 F g^{-1} (0.25 A g^{-1})	89.6% (Asy. 5000 cycles, 1.6 V, 1 A g^{-1})	Fan et al. (2014)
COP	202 F g^{-1} (1 A g^{-1})	84% (1000cycles, 1 V, 1A·g^{-1})	Feng et al. (2014)
COP + EOP	798 F g^{-1} (2 mV s^{-1})	77% (10,000 cycles, 1 V, 1 A g^{-1})	Lim et al. (2014)
COP	437 F g^{-1} (0.2 A g^{-1})	94.5% (10,000 cycles, 1 V, 5 A g^{-1})	Wu et al. (2014)
COP	253 F g^{-1} (0.5 A g^{-1})	93% (1000 cycles, 1.2 V, 10 A g^{-1})	Ye and Feng (2014)
COP	435 F g^{-1} (1 A g^{-1})	88% (5000 cycles, 1 V, 10 A g^{-1})	Yu et al. (2014)
COP	325 F g^{-1} (0.5 A g^{-1})	64% (500 cycles, 1 V, 50 mV s^{-1})	Fan et al. (2015)
EOP	224 F g^{-1} (240 A g^{-1})	83% (5000 cycles, 0.8 V, 30 A g^{-1})	Wang et al. (2012b)
EOP	237 F g^{-1} (10 mV s^{-1})		Davies et al. (2011)
EOP	356 F g^{-1} (0.5 A g^{-1})	78% (1000 cycles, 1 V, 100 mV s^{-1})	Zhu et al. (2012)
EOP	960 F g^{-1} (100 mV s^{-1})	100% (300 cycles, 0.6 V, 1 mA cm^{-2})	Chen et al. (2014)
EOP	660 F g^{-1} (0.5 mA cm^{-2})	90% (1000 cycles, 1 V, 10 mA cm^{-2})	Qi et al. (2014)
EOP	481 F g^{-1} (0.77 A g^{-1})	92% (2000 cycles, 0.8 V, 4 A g^{-1})	Cao et al. (2015)
EOP	196 mF cm^{-1} (1 mA cm^{-1})	90% (500 cycles, 1 V, 1 mA cm^{-1})	Yang et al. (2015b)

Capacitance—specific capacitance (charging/discharging rate), stability—retained capacitance (cycle number, voltage window, charging/discharging rate)

RGO usually prevent aggregation of GP sheets by strong polar–polar interactions or by their bulky size. In many cases, the adsorption of functional groups to GP sheet through π–π stacking and van der Waals interactions can aid its dispersion in a hydrophilic or hydrophobic media. There is no doubt that the functionalization and dispersion of GP sheets are very crucial to GP applications (Johnson et al. 2015; Kuila et al. 2012; Zhu et al. 2010).

GO dispersion

The groups on the surfaces of GO sheets, including hydroxyl, epoxide, diol, ketone, and carboxyl, can withstand the van der Waals interactions significantly and lead to a range of solubility in water and organic solvents. Therefore, it is relatively easy to prepare PPy/GO composites by in situ COP method (De Adhikari et al. 2015; Fan et al. 2014; Zhu et al. 2012), EOP method (Davies et al. 2011; Mini et al. 2011; Qi et al. 2014) and liquid/liquid interfacial polymerization (Bora and Dolui 2014) because pyrrole monomer, GO and other reagents can be evenly dispersed in liquid electrolyte by sonication without any surfactants. (Fan et al. 2014) synthesized the GO/PPy composites using in situ COP method. Pyrrole monomer, sodium p-toluenesulfonate and ammonium persulfate were added into GO solution, respectively, and stirred for polymerization. The mass ratios of GO to pyrrole in GO/PPy composites had a great effect on their electrochemical performance. When the mass ratios of GO to pyrrole is 1:10, the GO/PPy composite electrode showed the highest specific surface area of 98.6 m^2 g^{-1} and the highest capacitance of 332.6 F g^{-1} at a constant current density of 0.25 A g^{-1}. The specific capacitance obtained at a high current density of 2.5 A g^{-1} reached 82.5% of the value obtained at a low current density of 0.25 A g^{-1}, which can be resulted from high active surface, short diffusion path of ions, high electrical conductivity and intimate interfacial contact between PPy and GO.

On the contrary, many surfactants were used to obtain PPy/GO composites because composite structure became controllable in the presence of surfactants (Biswas and Drzal 2010; Feng et al. 2014; Li et al. 2013; Mao et al.

2012; Zhang et al. 2010, 2014). Zhang et al. (2010) considered that the morphology and electrochemical performance of PPy/GO composites can be controlled by varying the surfactant. The micelles of CTBA in aqueous solution interact with the GO sheets to form a GO-surfactant multilayer structure, leading to the formation of a layered GO structure with PPy fibers sandwiched either between GO sheets or on GO surfaces (GO/PPy-F). In the presence of surfactant dodecyltrimethylammonium bromide and solvent 1-decanol, spherical micelles induced the formation of the PPy spheres sandwiched between GO sheets (GO/PPy-S). This sandwich structure possesses many pores between GO sheets, by which ions in electrolyte can move freely. Therefore, the specific capacitance of GO/PPy-F and GO/PPy-S composites exceeded 500 F g^{-1} at a charging/discharging current density of 0.3 A g^{-1}. The GO/PPy-F composites retained 70% of its initial capacitance at a charging/discharging current density of 5 A g^{-1} after 10,000 cycles. In addition, GO/PPy nanowire composites were also fabricated with different mass ratio of GO to pyrrole nanowire by a soft template of CTBA (Li et al. 2013). A small content of GO in the composites enhanced both the specific capacitance and the rate capability. Though most of GO/PPy specific capacitance in available reports is less than 500 F g^{-1}, the specific capacitance of GP$_{5:95}$ (5:95, the mass ratio of GO to pyrrole nanowire) composite reached 728 F g^{-1} and 675 Ag^{-1} at a charging/discharging current density of 0.5 and 2.5 A g^{-1}, respectively. The GP$_{5:95}$ electrode exhibited a capacitive retention of about 93% at a CV scan rate of 50 mV s^{-1} after 1000 cycles. In conclusion, the higher specific capacitance and more homogeneous PPy/GO composites can be obtained in the presence of surfactants.

RGO dispersion

RGO is prepared by the reduction of GO and RGO properties is also closer to that of pristine GP (Pei and Cheng 2012). The dispersibility of RGO in aqueous solution is generally poor and aggregation occurs rapidly. However, there are still many methods to disperse RGO in aqueous solutions (Bora et al. 2014; Lai et al. 2012; Li et al. 2008; Wang et al. 2013; Zhang et al. 2011). These methods can be adopted to prepare PPy/RGO composites.

The surfactant CTBA can intercalate between GP sheets and inhibit aggregation of GP sheets during reduction (Mao et al. 2012). CTBA-stablilized RGO was obtained to synthesize PPy nanowire/RGO composites. As the mass ratio of PPy to CTBA-stablilized RGO in the composites was 9.46:1, a high specific capacitance of 492 F g^{-1} was obtained at a current density of 0.2 A g^{-1}. The presence of RGO sheets as a conductive material not only improved the electronic conductivity of composites but also induced a porous structure with a large surface area, which enhanced PPy utilization and ions transport during the charging/discharging processes.

Surface chemistry of GP is found to be of significant importance to GP diffusion, PPy growth and PPy/GP electrochemical performance improvement (Lai et al. 2012). Sulfonated GP (SG) with good dispersibility in aqueous solution prepared by anchoring the organic sulfonic acid on the surface of RGO nanosheets was used as the unique dopant for the in situ chemical polymerization of pyrrole (Wang et al. 2013). The SG sheets as both support and unique dopant were homogeneously coated on both surfaces by PPy films. As the mass ratio of PPy and SG in the composites was 1:0.258, the SG/PPy composite possessed the highest specific capacitance of 261.0 F g^{-1} at a charging/discharging current density of 1 A g^{-1}. About 87% of its original specific capacitance could be remained at a CV scan rate of 50 mV s^{-1} after 1000 cycles. Moreover, (Lai et al. 2012) prepared N-doped graphene/PPy (NG/PPy) electrode with a specific capacitance of 393.67 F g^{-1}, which is larger than those of GO/PPy, and RGO/PPy electrodes. The incorporation of N into the GP network enhanced electronic transfer efficiency and improved GP surface wettability, and thus largest synergistic effect is achieved in NG/PPy composites.

In addition, PPy/RGO composites were prepared by the reduction of as-prepared PPy/GO composites for avoiding RGO aggregation. Fan et al. prepared PPy/GO-CTAB composites and then the PPy/GO-CTAB composites were reduced into PPy/RGO-CTAB by vitamin C. The PPy/RGO-CTAB composite has specific capacitance of 324.8 F g^{-1} at a charging/discharging current density of 1 A g^{-1}, which is higher than 224.6 F g^{-1} of PPy/RGO, 170.3 F g^{-1} of PPy and 40.1 F g^{-1} of RGO. However, PPy/RGO-CTAB composites exhibited poor stability and the capacitance only retained 64% after 500 cycles. In addition, PPy/GO composites were also reduced into PPy/RGO by hydrazine (Liu et al. 2015). The flexible PPy/RGO films reduced by hydrazine showed an energy density of 13.15 mWh cm^{-3} while the power density is 1300 mW cm^{-3}. The specific capacitance of PPy/RGO composites that was prepared from the reduction of as-prepared PPy/GO composites should be enhanced further. PPy film on GO surface can interfere with GO reduction process, which causes the unsatisfactory electrochemical performance for PPy/RGO composite electrode.

3D PPy/graphene composites

With regard to electrochemical energy storage, the ideal electrode material should possess high surface area, stable structure, good ions and electron transport ability. The stable 3D network GP matrix should approach ideal electrode material. Several strategies were used for preparing 3D PPy/GP composites.

As shown in Fig. 8, the 3D GO/PPy composites were fabricated via a one-step electrochemical co-deposition method in aqueous solution containing pyrrole monomers, GO and $LiClO_4$ (Cao et al. 2015). The GO concentration had an important effect on controlling the morphologies of the GO/PPy composite electrodes. The unique 3D interconnected structure can be fabricated when the concentration of GO was a relatively low value of 0.1 mg mL^{-1}. The 3D GO/PPy composites exhibited the highest specific capacitance of 481.1 F g^{-1} at a charging/discharging current density of 0.2 mA cm^{-2} as loading a small mass GO/PPy composites of 0.26 mg cm^{-2}. The capacitance maintained 92.1 and 84.8% of its initial capacitance at a charging/discharging current density of 0.2 mA cm^{-2} after 2000 and 5000 cycles, respectively. In the work of (Yang et al. 2015a), the 3D macroporous GP/PPy (MG/PPy) electrode was prepared using hydrogen bubbles as the dynamic template. The MG/PPy composites were constructed via directly electropolymerization onto modified GP electrode in aqueous electrolyte containing pyrrole monomer and sodium dodecylbenzenesulfonate. The results indicated that the morphology and pore size of 3D modified GP could be controlled by the concentration of surfactants, electrodeposition time, and applied voltage. Noting that MG/PPy composites after thermal treatment at 800 °C for 2 h exhibited excellent catalytic performance toward the oxygen reduction in proton exchange membrane fuel cells. A 3D hierarchical GP/PPy aerogel (GP/PA) has

been fabricated via GO and PPy nanotubes reacting in seal glass vials at 95 °C for 4 h (Ye and Feng 2014). PPy nanotubes not only provide a large accessible surface area for fast transport of hydrate ions but also act as spacers to prevent the restacking of graphene sheets. The supercapacitor electrodes based on GP/PA exhibited a highest specific capacitance up to 253 F g^{-1} at a current density of 0.5 A g^{-1} and the capacitance retention reached 93% at a current density of 10 A g^{-1} after 2000 cycles. Unexpectedly, the GP/PA exhibited satisfactory mechanical strength and press-resistance. For example, a dried GP/PA monolith ($\sim$20 mg) can support at over 5000 times of its own weight without collapsing.

In addition, as shown in Fig. 9, PPy/GO nanowires are prepared via electrodepositing in a microporous Al_2O_3 template (Chen et al. 2014). This structure is similar to VA-CNTs with vertical alignment active material that has a large surface area allowing a fast transport of electron and ions. A very high specific capacitance 960 F g^{-1} of the GO/PPy nanowires was obtained at a CV scan rate of 100 mV s^{-1}. The specific capacitance of 960 F g^{-1} is the highest value of PPy composites with carbon materials in available reports, which should be closely related to a high specific surface area.

In conclusion, 3D PPy/GP composites exhibited high specific capacitance and charging/discharging rate in available reports. However, the junction of different materials in 3D network structure is easy to be damaged

Fig. 8 **a**, **b** Surface SEM morphology of the GO/PPy composite electrode. **c** Photograph of a Ti foil coated with the GO/PPy composite film. **d**, **e** Cross-sectional SEM morphology of the GO/PPy composite film. **f** TEM image of PPy-coated GO sheets
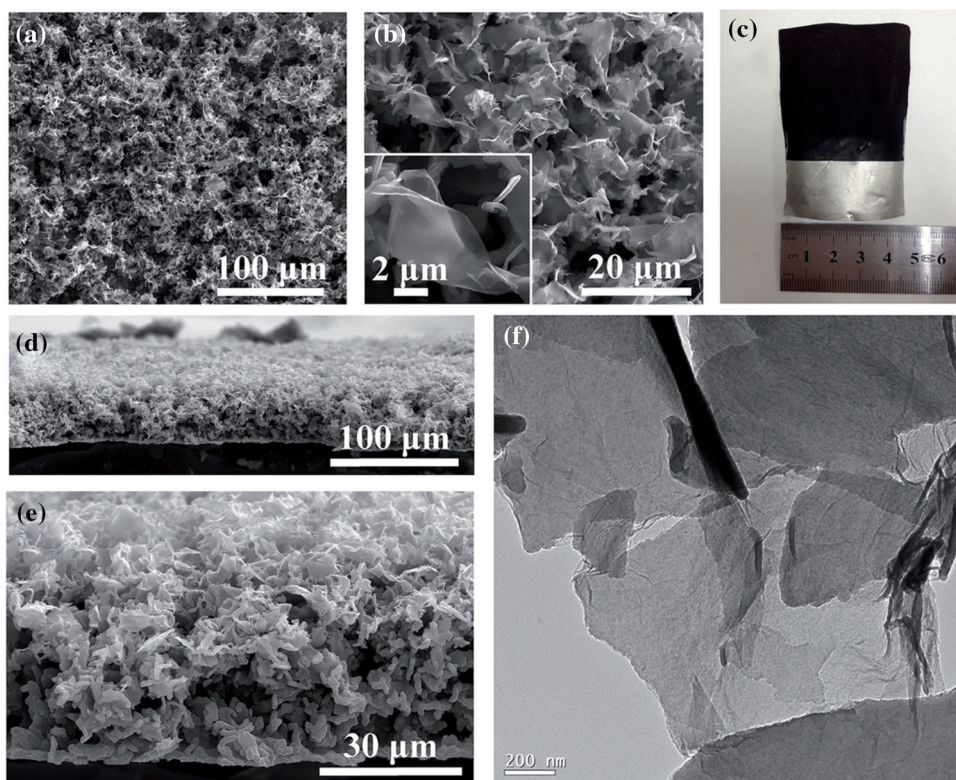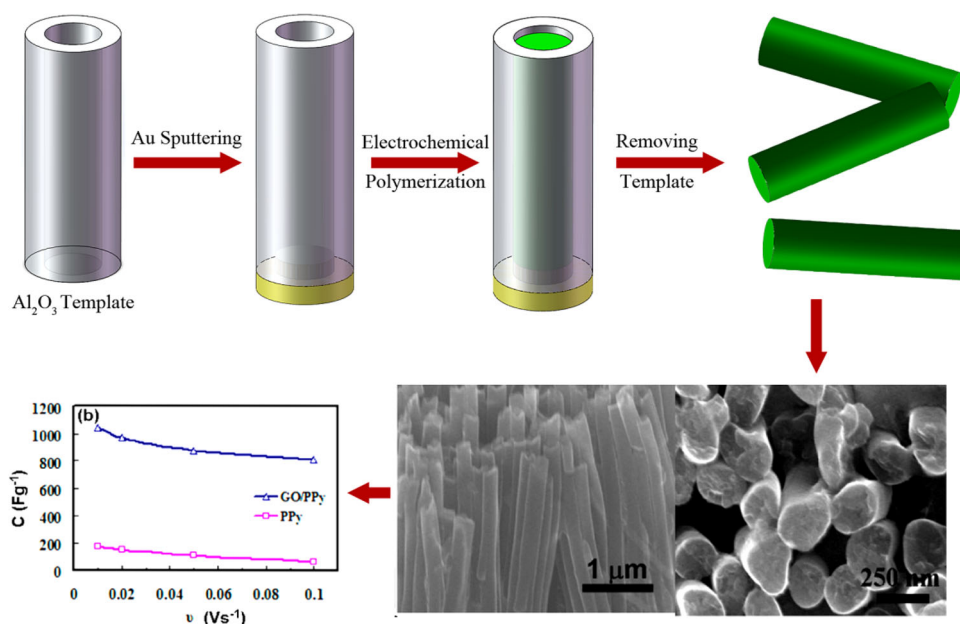
Fig. 9 Schematic of the fabrication process of PPy/GP nanowires

when the shrinkage and expansion of PPy active material occur for many times, which can cause the collapse of 3D network structure. Therefore, the stability of 3D network structure should be explored further in the future.

PPy/graphene application in flexible supercapacitors

The flexible supercapacitors and battery were prepared using various composites, which contains PPy/GP composites. In available reports, the flexible electrode of PPy/GP composites mainly contains two forms: fiber-shaped Ding et al. (2014) and plate-shaped electrodes (Chen et al. 2015a; Davies et al. 2011; Liu et al. 2015; Yu et al. 2014).

(Ding et al. 2014) developed a facile approach for fabricating of PPy/GP composite fibers via a wet-spinning strategy, which is an imaginative method. The mixture composed of GO aqueous dispersion and pyrrole monomer was directly spun in an aqueous $FeCl_3$ solution using a single capillary needle, in which pyrrole was polymerized to PPy and accordingly the PPy/GO fibers are continuously produced into the solution. The PPy/GO fibers were reduced into PPy/GP by chemical reduction and fiber diameter can be controlled in the range of about 15–80 mm. The fibers exhibited high conductivity (137–144 S m^{-1}), good flexibility and elasticity to intertwine as intended. In the test of flexible all-solid-state fiber supercapacitors, a stable capacitance of 95–105 mF cm^{-2} (65–72 F g^{-1}) was obtained at a current density of 0.15 mA cm^{-2} during 1000 cycles.

In the case of the plate-shaped electrode, PPy/GP composites were anchored on a soft substrate using electrophoretic deposition (EPD) (Liu et al. 2015),

electrodeposition (Davies et al. 2011) or natural adsorption (Chen et al. 2015a; Yu et al. 2014). Figure 10 exhibits the structure of flexible supercapacitors with a plate-shaped structure, which was prepared using PPy/RGO to coat on polyethylene terephthalate substrate with Nickel plated conductive fabric (Yu et al. 2014). All-solid-state flexible supercapacitors based on PPy/RGO composites showed a specific capacitance of 434.7 F g^{-1} at a current density of 1 A g^{-1} and retained 88.1% initial capacity after 5000 cycles. This all-solid-state flexible supercapacitor showed the similar electrochemical performances under different bending angles. (Davies et al. 2011) obtained a uniform GP film on a polycarbonate membrane through a vacuum filter. The electrodeposition with a pulse current was carried out using GP film as working electrode in an aqueous solution containing pyrrole monomer. The highest specific capacitances 237 F g^{-1} were achieved at a CV scan rate of 10 mV s^{-1}. The flexible film exhibited high energy of $\sim$33 Wh kg^{-1} and power densities of $\sim$1184 W kg^{-1}, respectively, at a CV scan rate of 10 mV s^{-1}. The pulse electrodeposition allows pyrrole monomer to diffuse into the intercalating spaces between GP sheets at pulse off time and to be electropolymerized at pulse on time. The pulse electrodeposition can cause a uniform deposition of PPy on the GP sheet. In addition, the plate-shaped electrode based on PPy/RGO composites has been fabricated by a simple EPD technique (Liu et al. 2015). This electrode using PVA-H$_2$SO$_4$ as electrolyte demonstrated high volumetric capacitance of 147.9 F cm^{-3}, high energy density of 13.15 mWh cm^{-3} at a power density of 1300 mWh cm^{-3}. The supercapacitors retained approximately 71.7% of the initial capacitance after 5000 cycles.

Fig. 10 Schematic diagram of flexible plate-shaped supercapacitors with PVA-H$_2$SO$_4$ polymer gel as electrode

1 ▉ Poly(ethylene terephthalate)
2 ▉ Nickel plated conductive fabric
3 ▉ V-PPy/RGO
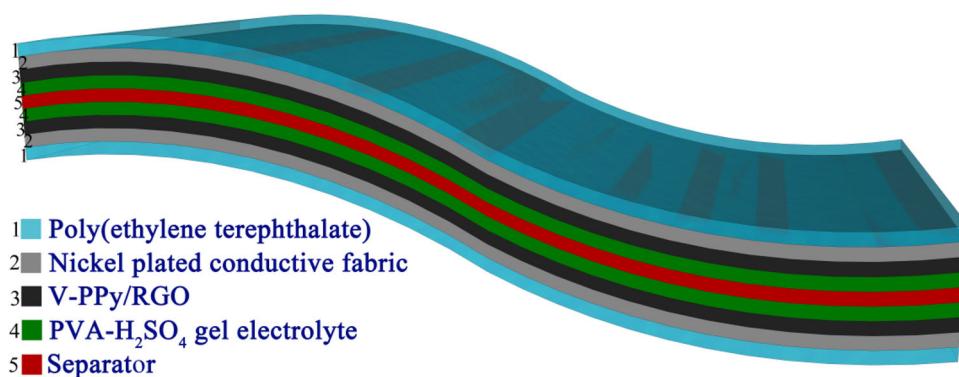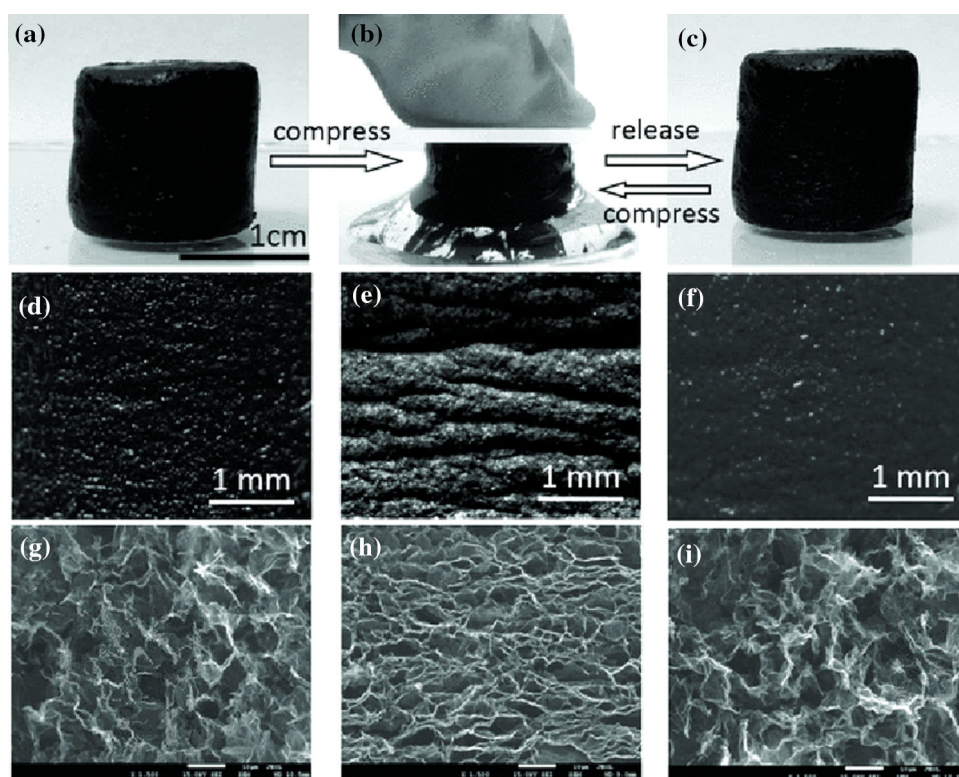4 ▉ PVA-H$_2$SO$_4$ gel electrolyte
5 ▉ Separator

Fig. 11 **a–c** Compression-recovery processes of PPy-G foam. **d–f** Surface views of PPy-G foam corresponding to the unloading-loading-unloading status in **a–c**, respectively. **g–i** SEM images of the inner microstructures of PPy-G foam corresponding to the loading–unloading status in **a–c**, respectively

Noting that highly compressible supercapacitors were fabricated using PPy/GP foam as electrode, as shown in Fig. 11 (Zhao et al. 2013). The specific capacitance of PPy/GP foam reached 350 F g^{-1} at a current density of 1.5 A g^{-1}. The assembled supercapacitor based on this foam electrodes achieved superb compression tolerance without significant variation of capacitances under long-term compressive loading and unloading processes, showing that no significant change was observed in the CVs of the compressed supercapacitors with a 50% applied strain, which is also the case for 1000 measured cycles. The as-formed PPy/GP foam was durably tolerant to the large compressive strain without any structural collapse and loss of springiness. As the deformable electrodes for assembly of highly compression-tolerant supercapacitors, PPy/GP foam performed high specific capacitances without significant variation under long-term compressively loading and unloading process.

Composites of PPy/other carbon materials for supercapacitors

Due to the wide range of carbon materials, PPy composites with other carbon materials have been also fabricated for supercapacitors. Meanwhile, the composites containing PPy and various carbon materials were prepared for supercapacitors. Table 3 shows the electrochemical performances of other PPy/carbon materials composites.

Table 3 Description of PPy/other carbon materials

Synthesis	Capacitance	Stability	References
EOP (PPy/AC)	354 F g^{-1} (1 mV s^{-1})		Muthulakshmi et al. (2006)
COP (PPy/C)	395 F g^{-1} (50 mV s^{-1})	100% (500 cycles, 1 V, 100 mV s^{-1})	Kumar et al. (2014)
COP (PPy/CB)	366 F g^{-1} (5 mA cm^{-2})	95% (100 cycles, 1 V, 5 mA cm^{-2})	Yang et al. (2011)
COP (PPy/CA)	433 F g^{-1} (1 mV s^{-1})	50% (1000 cycles, 1 V, 1 A g^{-1})	An et al. (2010)
COP (CNC/PPy-NFs)	3.32 m F cm^2 (2 mV s^{-1})	84.19% (2000 cycles, 0.9 V, 0.1 A cm^{-2})	Yang et al. (2015c)
EOP (PPy/CFs)	460 ± 50 F g^{-1} (4.3 A g^{-1})	87% (1000 cycles, 1.4 V, 100 mV s^{-1})	Davoglio et al. (2013)
COP (PPy/GN/CNT)	361 F g^{-1} (0.2 A g^{-1})	96% (2000 cycles, 1 V, 6 A g^{-1})	Lu et al. (2012b)
EOP (PPy/GN/CNT)	453 F g^{-1} (5 mV s^{-1})		Aphale et al. (2015)
COP (PPy/GO/CNF)	144.6 F g^{-1} (10 mV s^{-1})	89% (5000 cycles, 0.8 V, 1 A g^{-1})	Xu et al. (2014)
EOP (CNF@G/PPy)	386 F g^{-1} (2 mV s^{-1})	84% (1000 cycles, 0.9 V, 2 A g^{-1})	Gan et al. (2015)

Capacitance—specific capacitance (charging/discharging rate), stability—retained capacitance (cycle number, voltage window, charging/discharging rate)

Binary composites

Carbon gels, in particular CA, are porous materials that have received and continue to attract attention in the literatures and in potential commercial applications due to high electrical conductivity, low density and high specific surface area since they were first reported by Pekala in 1989 (White et al. 2014). The PPy/CA composites containing different PPy contents are prepared by chemical oxidation polymerization for supercapacitor electrode (An et al. 2010). The PPy/CA composites exhibited high specific capacitance of 433 F g^{-1} at a CV scan rate of 1 mV s^{-1}, which is much higher than that of pure CA. In the test of long-term cycling life, the loss of PPy/CA capacitance was large during initial 500 cycles possibly due to PPy instability, but the capacitance stabilized at a fixed value after 500 cycles. Moreover, the cellulose nanocrystals aerogels can act as the substrates for a nano-sized composites, containing PPy nanofibers (PPy-NFs), PPy-coated carbon nanotubes (PPy-CNTs) and spherical manganese dioxide nanoparticles (MnO$_2$-NP) during the aerogel assembly (Yang et al. 2015c). The preparation process of cellulose nanocrystals aerogels is shown in Fig. 12. The aerogels are so lightweight that they can rest on top of a feather and exhibited similar internal morphology. The specific capacitance at a CV scan rate of 2 mV s^{-1} for PPy-NFs, PPy-CNTs, and MnO$_2$-NP devices was 3.32, 2.42, and 2.14 mF cm^{-2}, respectively. The symmetric supercapacitor cells showed 84.19, 61.66, and 92.28% capacitance retention at a current density of 0.1 mA cm^{-2} after 2000 cycles for PPy-NFs, PPy-CNTs, and MnO$_2$-NP, respectively. If the 3D aerogel structure with a large specific area can utilize for charge storage, a high specific capacitance should be obtained.

CFs was often used to reinforce polymer for high conductivity and stability (Davoglio et al. 2010; Izadi-Najafabadi et al. 2005). The PPy/CFs and PPy/poly (2,5-dimercapto-1,3,4-thiadiazole)/CFs (PPy/P(DMcT)/CFs) composites were prepared using EOP method as supercapacitor electrodes, respectively (Davoglio, Biaggio, Bocchi and Rocha-Filho 2013). P(DMcT) is one of the most promising candidates due to its high theoretical specific energy (1080 Wh kg^{-1}) and high stability to temperature (NuLi, Guo, Liu and Yang 2007). Unfortunately, its redox kinetics is rather slow at room temperature and it is not electrically conducting, which may lead to significantly lower power density (Li et al. 2003). However, when P(DMcT) was coated by PPy films, the bilayer polymer material presented a significantly greater specific capacitance of 1130 ± 100 F g^{-1}. After 1000 cycles, only about 17% of the initial capacitance were lost for PPy/P(DMcT)/CFs electrodes, respectively. A thin film of electrodeposited PPy is enough to prevent the degradation of the inner poly(DMcT) layer. An important synergic effect should exist between both polymers. In addition, the PPy/CFs composites were also used as the precursor to prepare nitrogen-doped carbon nanofibers (N-CNFs) for supercapacitor electrode (Cai et al. 2015a; Chen et al. 2012). The PPy/carbonaceous nanofibers composites were prepared via a chemical oxidation polymerization, and then annealed in quartz tube under N$_2$ atmosphere for heating at 500, 700, 900, and 1100 °C to obtain N-CNFs (Chen et al. 2012). The precursors used in the process can be synthesized on large-scale or are commercially available. The N-CNFs nanofibers exhibited a reversible specific capacitance of 202.0 F g^{-1} at the current density of 1 A g^{-1} in 6.0 mol L^{-1} aqueous KOH electrolyte, meanwhile, maintaining 97% of the initial capacitance after 3000 cycles. In the work of Cai et al. (2015a), the N-CNFs nanofibers can be further activated in CO$_2$ atmosphere at 850 °C for 2 h, by which the capacitance of N-CNFs electrodes were enhanced obviously. The preparation process of active
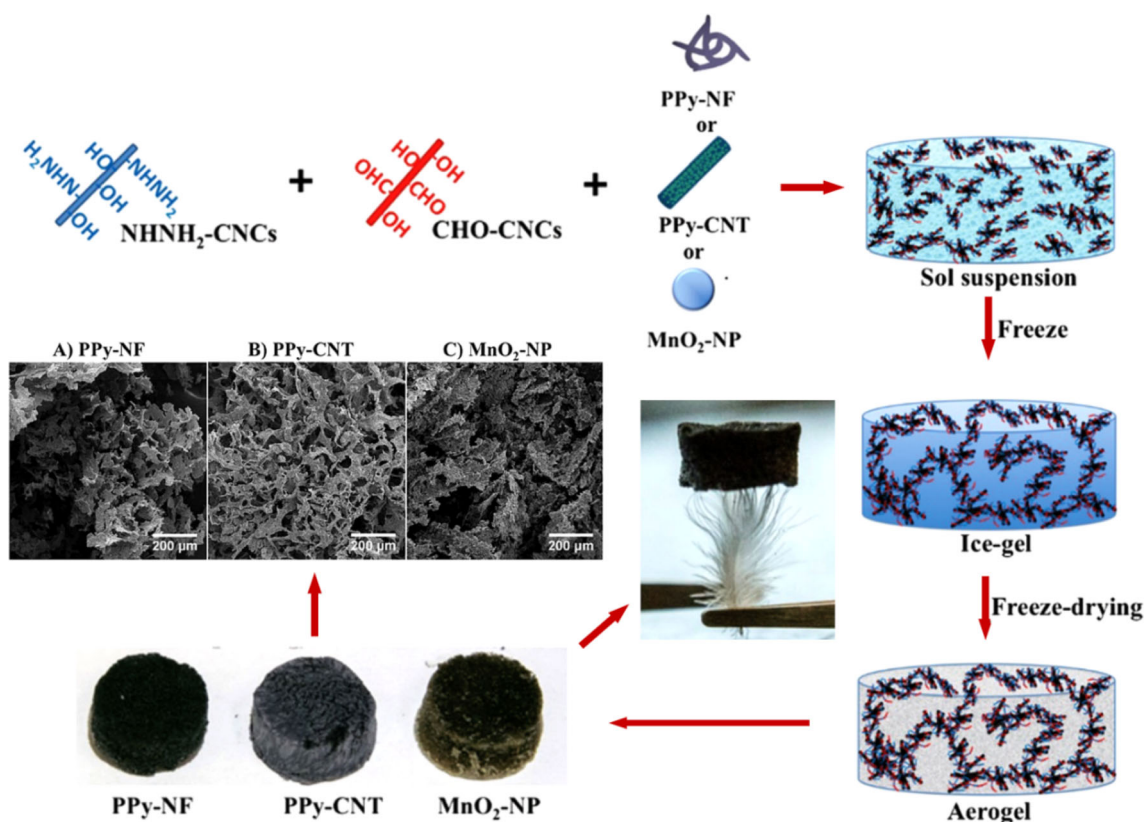
Fig. 12 Schematic representation for preparation process of cellulose nanocrystals aerogels

N-CNFs nanofibers is shown in Fig. 13. Supercapacitor electrodes prepared from N-CNFs and a mixture of N-CNF and Ni(OH)$_2$ showed the specific capacitance of 236 and 1045 F g^{-1} at a current density of 0.2 A g^{-1}, respectively. An asymmetric supercapacitor using N-CNF/Ni(OH)$_2$ and N-CNFs as positive and negative electrodes exhibited the high energy density of 51 Wh kg^{-1} and power density of 117 kW kg^{-1}. The device retained 84% of the initial value at a CV scan rate of 100 mV s^{-1} after the initial 5000 scan cycles.

As the most common electrode materials for commercially available supercapacitors, AC has a high cycling life and low cost, while its electrical conductivity and capacitance value are lower than PPy active materials. So, PPy/AC composites were fabricated using in situ EOP and exhibited a high specific capacitance of 354 F g^{-1} at a CV scan rate of 1 mV s^{-1}, which indicated that AC coated by PPy can improve the performance of AC electrode in supercapacitors (Muthulakshmi et al. 2006). The PPy/conductive carbon black (PPy/CCB) composites were prepared via in situ COP to develop an electrode material for supercapacitors (Kumar et al. 2014). The results indicated that the concentration of dopant anion (*p*-toluenesulfonic anion) can impact the conduction channel inside PPy/CCB matrix through the formation of bipolaronic and polaronic species for effective transfer of charges across the electrode/electrolyte interface. The maximum specific capacitance of PPy/CCB composites reached 395 F g^{-1} at a CV scan rate of 50 mV s^{-1} in 0.5 M Na$_2$SO$_4$ aqueous solution and demonstrated good stability during 500 cycles. Moreover, PPy/core–shell carbon black (PPy/CB) composites were prepared via in situ COP with poly[2-hydroxy-3-(methacryloyloxy) propane-1-sulfonate] (PHMAS) as both surfactant and dopant (Yang et al. 2011). The maximum specific capacitance of PPy/CB composites reached 366 F g^{-1} at a current density of 5 mA cm^2. It was found that a total loss of about 5–12% of the initial discharge capacitance was observed after 40 cycles, but a fairly stable capacitance was maintained thereafter.

Ternary composites

To excellent electrochemical performance, PPy electrodes were reinforced by two kinds of carbon material (Gan et al. 2015; Lu et al. 2012a; Peng et al. 2014; Shi and Zhitomirsky 2013a; Wu et al. 2014; Xu et al. 2014; Yang et al. 2014; Zhang et al. 2015). These structures are similar to beton matrix and PPy acts as binder. On the other hand, two kinds of carbon materials can introduce more pores to ion transfer in composites matrix. Both the fast faradaic
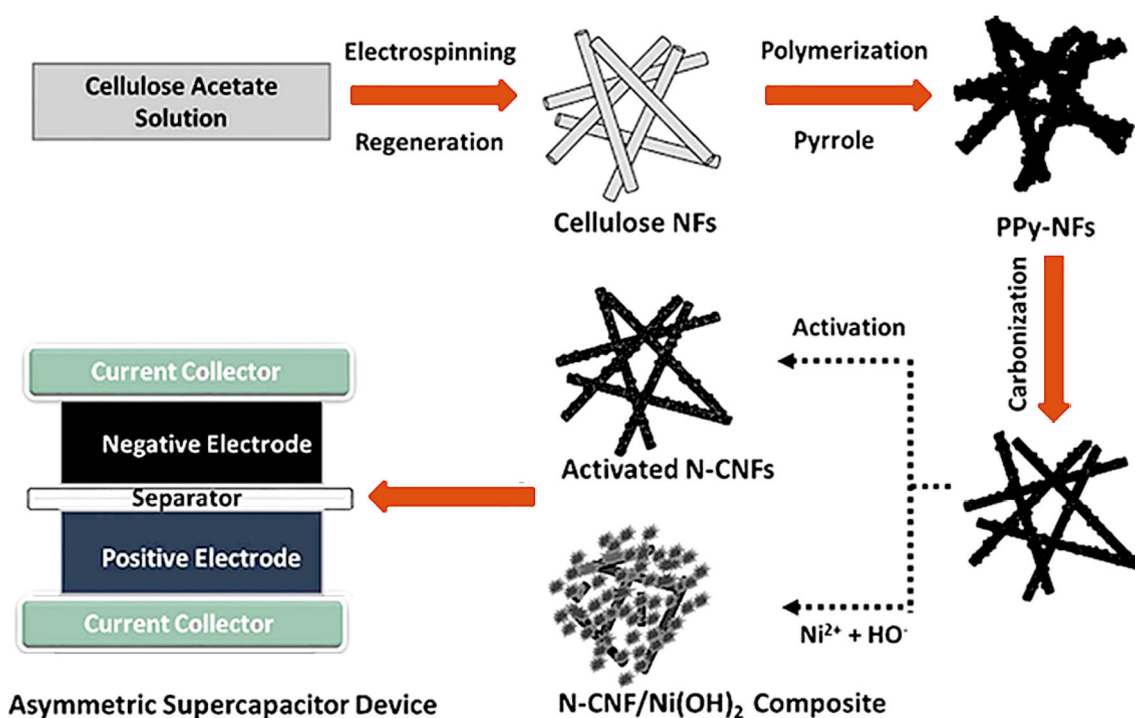
Fig. 13 Schematic representation for preparation process of N-CNFs and a mixture of N-CNF and Ni(OH)$_2$

capacitance and reversible double-layer capacitance at the electrode–electrolyte interfaces can be obtained in these novel composites. The composites can show good cycleability owing to two kinds of carbon materials synergistically accommodating the strain of PPy volume change (Lu et al. 2012a).

Lu et al. (2012b) prepared the functionalized GP and CNTs using negatively charged poly(sodium 4-styrenesulfonate), and then fabricated PPy/GN/CNT composites via in situ COP. The PPy/GN/CNT composites exhibited a large surface area of 112 m^2 g^{-1} and meso- and macro-porosity system. The maximum specific capacitance of composites reached 361 F g^{-1} at a current density of 0.2 A g^{-1}, which is much higher than that of pure PPy (176 F g^{-1}) and binary composites of CNT/PPy (253 F g^{-1}) and GN/PPy (265 F g^{-1}). Owing to the GN and CNTs synergistically releasing the intrinsic strain of PPy chains during charging/discharging processes, the PPy/GN/CNT composite retained 96% of its initial capacitance after 2000 charging/discharging cycles at a current density of 6 A g^{-1}. Meanwhile, PPy/GP/CNTs composites can be fabricated via in situ potentiostatic electrochemical polymerization (Aphale et al. 2015). To PPy/GP/CNTs EOP, no organic binders were used to fabricate the thin film, which would increase the ionic access to the active materials in the supercapacitor electrodes. At a scan rate of 5 mV s^{-1}, the specific capacitance, energy and power density of PPy/GP/CNTs electrode prepared via EOP reached 453 F g^{-1}, 62.96 and 566.66 W kg^{-1}, respectively.

The supercritical carbon dioxide was used to prepare unique flexible free-standing graphene oxide/carbon nanofiber films (GO/CNF), on which PPy was deposited via an in situ COP (Xu et al. 2014). The foam carbon nanofiber with core–shell architecture (CNF/GP/PPy) was fabricated via a two-step method, containing electrospinning and potentiostatic electrodeposition (Gan et al. 2015). The carbon nanofibers acted as an electrically conductive substrate that enables the incorporation of the GP/PPy shell. The GP addition decreased the charge transfer resistance possibly due to reducing the distance for electron shuttling in the PPy chains for rapid electrochemical redox reactions. The specific capacitance of CNF/GP/PPy reached 386 F g^{-1} at a CV scan rate of 2 mV s^{-1}. They considered that GO can be reduced to GP in the presence of the pyrrole monomer during electrodeposition process because the negatively charged GO is attracted to the oligomer radical cations due to electrostatic charge attraction, and is subsequently reduced to GP by the free electrons released during the formation of free radicals (Gan et al. 2015).

Conclusion

As supercapacitor electrodes, PPy offers many advantages, such as high conductivity, flexible structure, low cost and easily preparing process. However, the big volume change of PPy electrode resulted from the unavoidable doping/

dedoping process induces defects into PPy matrix. So the intrinsic PPy has a poor cyclic stability while compared with carbon materials that only involve simple ion absorption and desorption on materials interface. Based on the available reports, carbon materials, especially GP and CNTs, are very suitable to reinforce PPy electrodes during repeatedly charging/discharging process. So many PPy/carbon material composites were prepared with different structure or component. Though few works can meet the level of supercapacitors in practical application, the various strategies in available literatures improved their electrochemical performance from different angles, which has to benefit PPy commercial application.

The PPy/carbon material composites with 3D porous matrix exhibited high specific capacitance and charging/discharging rate. This structure provides a high specific surface area for electrolyte contacting with active material and reduces "dead" material as far as possible. The 3D porous matrix allows a high loading active material, which plays a crucial role in practical application. An appropriate distribution range of pore diameter is very critical to the electrochemical performance of composites because the pore diameter determines whether the electrolyte adequately contact with the surface of active materials. Therefore, the 3D porous structure of composites should be optimized seriously. The 3D porous composites usually were fabricated by several strategies, such as the use of sacrificial template, the use of a reinforcing material with a 3D structure, and preparing the sponge and foam composites by various unique process. Currently, a simple and low cost method to fabricate 3D porous PPy/carbon material composites should be very important to PPy commercial application.

PPy possesses good flexibility when PPy was polymerized by a suitable process. The flexible PPy can be prepared by the simple methods. PPy/carbon material composites meet the most demands of energy storage device in wearable electronics area. Therefore, many researchers focused on the preparation and application of PPy/carbon material composites for the flexible supercapacitors. However, for the commercialization, material stability, compatibility and cost need to be resolved. In addition, towards many practical applications, multifunctional flexible electrode materials can be more popular in the future. It can be expected that the multifunctional PPy/carbon material composites are used in wearable electronics, bio-implantable devices, flexible and wireless sensors.

The asymmetric supercapacitors are assembled with different material at positive and negative electrodes. This configuration can enlarge the working potential window and enhance the high energy density. In the symmetric supercapacitors, when PPy was reduced, it has a poor conductivity due to low doping level, as shown in Fig. 2. This should increase sharply the internal resistance of supercapacitors. Therefore, PPy and its composites are suited to be used as positive electrode in asymmetric supercapacitors. At the same time, the balance of thickness and mass of active materials on positive and negative electrodes has an important effect on the electrochemical performance. If electrodes are not matched, its performance may drop or the capacitance may be damaged. Therefore, matching electrodes should be carefully considered when PPy/carbon material composites were used in asymmetric supercapacitors.

In regard to cycling stability, there was still a gap between most of PPy/carbon material composites in available literatures and electrode materials of commercial supercapacitors. During repeatedly charging/discharging process, it is still unclear what cause the capacitance decay of these composites. The interface between PPy and carbon materials, the change of PPy intrinsic structure, and the change of porous structure need to be explored further during long-term cycle process.

References

An H, Wang Y, Wang X, Zheng L, Wang X, Yi L, Zhang X (2010) Polypyrrole/carbon aerogel composite materials for supercapacitor. J Power Sources 195(19):6964–6969. doi:10.1016/j.jpowsour.2010.04.074

An B, Xu S, Li L, Tao J, Huang F, Geng X (2013) Carbon nanotubes coated with a nitrogen-doped carbon layer and its enhanced electrochemical capacitance. J Mater Chem A 1(24):7222–7228. doi:10.1039/c3ta10830a

Aphale A, Maisuria K, Mahapatra MK, Santiago A, Singh P and Patra P (2015) Hybrid electrodes by in-situ integration of graphene and carbon-nanotubes in polypyrrole for supercapacitors. Sci Reports 5. doi:10.1038/srep14445

Aradilla D, Gaboriau D, Bidan G, Gentile P, Boniface M, Dubal D, Sadki S (2015) An innovative 3-D nanoforest heterostructure made of polypyrrole coated silicon nanotrees for new high performance hybrid micro-supercapacitors. J Mater Chem A 3(26):13978–13985. doi:10.1039/c5ta03435c

Arcila-Velez MR, Roberts ME (2014) Redox solute doped polypyrrole for high-charge capacity polymer electrodes. Chem Mater 26(4):1601–1607. doi:10.1021/cm403630h

Ata MS, Zhitomirsky I (2015) Colloidal methods for the fabrication of carbon nanotube-manganese dioxide and carbon nanotube-polypyrrole composites using bile acids. J Colloid Interface Sci 454:27–34. doi:10.1016/j.jcis.2015.05.014

Baronetto D, Krstajić N, Trasatti S (1994) Reply to "note on a method to interrelate inner and outer electrode areas" by H. Vogt. Electro Acta 39(16):2359–2362. doi:10.1016/0013-4686(94)E0158-K

Biswas S, Drzal LT (2010) Multi layered nanoarchitecture of graphene nanosheets and polypyrrole nanowires for high performance supercapacitor electrodes. Chem Mater 22(20):5667–5671. doi:10.1021/cm101132g

Bora C, Dolui SK (2014) Interfacial synthesis of polypyrrole/graphene composites and investigation of their optical, electrical and electrochemical properties. Polym Int 63(8):1439–1446. doi:10.1002/pi.4635

Bora C, Sharma J, Dolui S (2014) Polypyrrole/Sulfonated graphene composite as electrode material for supercapacitor. J Phys Chem C 118(51):29688–29694. doi:10.1021/jp511095s

Borchardt L, Oschatz M, Kaskel S (2014) Tailoring porosity in carbon materials for supercapacitor applications. Mater Horiz 1(2):157–168. doi:10.1039/C3MH00112A

Brownson DAC, Kampouris DK, Banks CE (2011) An overview of graphene in energy production and storage applications. J Power Sources 196(11):4873–4885. doi:10.1016/j.jpowsour.2011.02.022

Cai J, Niu H, Li Z, Du Y, Cizek P, Xie Z, Lin T (2015a) High-performance supercapacitor electrode materials from cellulose-derived carbon nanofibers. ACS appl mater interfaces 7(27):14946–14953. doi:10.1021/acsami.5b03757

Cai X, Hansen RV, Zhang L, Li B, Poh CK, Lim SH, Shen Z (2015b) Binary metal sulfides and polypyrrole on vertically aligned carbon nanotube arrays/carbon fiber paper as high-performance electrodes. J Mater Chem A 3(44):22043–22052. doi:10.1039/c5ta05961e

Cao J, Wang Y, Chen J, Li X, Walsh FC, Ouyang J-H, Zhou Y (2015) Three-dimensional graphene oxide/polypyrrole composite electrodes fabricated by one-step electrodeposition for high performance supercapacitors. J Mater Chem A 3(27):14445–14457. doi:10.1039/c5ta02920a

Chandra A, Roberts AJ, Lam How Yee E, Slade RC (2009) Nanostructured oxides for energy storage applications in batteries and supercapacitors. Pure Appl Chem 81(8):1489–1498. doi:10.1351/PAC-CON-08-08-20

Chen S, Zhitomirsky I (2013) Influence of dopants and carbon nanotubes on polypyrrole electropolymerization and capacitive behavior. Mater Lett 98:67–70. doi:10.1016/j.matlet.2013.01.123

Chen S, Zhitomirsky I (2014) Polypyrrole coated carbon nanotubes for supercapacitors, prepared using indigo carmine as a dispersant and dopant. Mater Lett 135:47–50. doi:10.1016/j.matlet.2014.07.113

Chen L-F, Zhang X-D, Liang H-W, Kong M, Guan Q-F, Chen P, Yu S-H (2012) Synthesis of nitrogen-doped porous carbon nanofibers as an efficient electrode material for supercapacitors. ACS Nano 6(8):7092–7102. doi:10.1021/nn302147s

Chen Z, Yu D, Xiong W, Liu P, Liu Y, Dai L (2014) Graphene-based nanowire supercapacitors. Langmuir 30(12):3567–3571. doi:10.1021/la500299s

Chen H, Zeng S, Chen M, Zhang Y, Li Q (2015a) Fabrication and functionalization of carbon nanotube films for high-performance flexible supercapacitors. Carbon 92:271–296. doi:10.1016/j.carbon.2015.04.010

Chen Y, Du L, Yang P, Sun P, Yu X, Mai W (2015b) Significantly enhanced robustness and electrochemical performance of flexible carbon nanotube-based supercapacitors by electrodepositing polypyrrole. J Power Sources 287:68–74. doi:10.1016/j.jpowsour.2015.04.026

Chen Y, Han M, Tang Y, Bao J, Li S, Lan Y, Dai Z (2015c) Polypyrrole-polyoxometalate/reduced graphene oxide ternary nanohybrids for flexible, all-solid-state supercapacitors. Chem Commun 51(62):12377–12380. doi:10.1039/c5cc02717a

Davies A, Audette P, Farrow B, Hassan F, Chen Z, Choi J-Y, Yu A (2011) Graphene-based flexible supercapacitors: pulse-electropolymerization of polypyrrole on free-standing graphene films. J Phys Chem C 115(35):17612–17620. doi:10.1021/jp205568v

Davoglio RA, Biaggio SR, Rocha RC, Bocchi N (2010) Bilayered nanofilm of polypyrrole and poly(DMcT) for high-performance battery cathodes. J Power Sources 195(9):2924–2927. doi:10.1016/j.jpowsour.2009.11.014

Davoglio RA, Biaggio SR, Bocchi N, Rocha-Filho RC (2013) Flexible and high surface area composites of carbon fiber, polypyrrole, and poly(DMcT) for supercapacitor electrodes. Electrochim Acta 93:93–100. doi:10.1016/j.electacta.2013.01.062

De Adhikari A, Oraon R, Tiwari SK, Lee JH, Nayak GC (2015) Effect of waste cellulose fibres on the charge storage capacity of polypyrrole and graphene/polypyrrole electrodes for supercapacitor application. RSC Adv 5(35):27347–27355. doi:10.1039/c4ra16174b

Debiemme-Chouvy C, Tran TTM (2008) An insight into the overoxidation of polypyrrole materials. Electrochem Commun 10(6):947–950. doi:10.1016/j.elecom.2008.04.024

Ding X, Zhao Y, Hu C, Hu Y, Dong Z, Chen N, Qu L (2014) Spinning fabrication of graphene/polypyrrole composite fibers for all-solid-state, flexible fibriform supercapacitors. J Mater Chem A 2(31):12355–12360. doi:10.1039/c4ta01230e

Dubal DP, Lee SH, Kim JG, Kim WB, Lokhande CD (2012) Porous polypyrrole clusters prepared by electropolymerization for a high performance supercapacitor. J Mater Chem 22(7):3044–3052. doi:10.1039/c2jm14470k

Fan J, Wan M, Zhu D, Chang B, Pan Z, Xie S (1999a) Synthesis and properties of carbon nanotube-polypyrrole composites. Synth Met 102(1–3 pt 2):1266–1267. doi:10.1016/S0379-6779(98)01462-3

Fan J, Wan M, Zhu D, Chang B, Pan Z, Xie S (1999b) Synthesis, characterizations, and physical properties of carbon nanotubes coated by conducting polypyrrole. J Appl Polym Sci 74(11):2605–2610. doi:10.1002/(SICI)1097-4628(19991209)74:11<2605:AID-APP6>3.0.CO;2-R

Fan L-Q, Liu G-J, Wu J-H, Liu L, Lin J-M, Wei Y-L (2014) Asymmetric supercapacitor based on graphene oxide/polypyrrole composite and activated carbon electrodes. Electrochim Acta 137:26–33. doi:10.1016/j.electacta.2014.05.137

Fan X, Yang Z, He N (2015) Hierarchical nanostructured polypyrrole/graphene composites as supercapacitor electrode. RSC Adv 5(20):15096–15102. doi:10.1039/c4ra15258a

Fang Y, Liu J, Yu DJ, Wicksted JP, Kalkan K, Topal CO, Li J (2010) Self-supported supercapacitor membranes: polypyrrole-coated carbon nanotube networks enabled by pulsed electrodeposition. J Power Sources 195(2):674–679. doi:10.1016/j.jpowsour.2009.07.033

Feng HX, Wang B, Tan L, Chen NL, Wang NX, Chen BY (2014) Polypyrrole/hexadecylpyridinium chloride-modified graphite oxide composites: fabrication, characterization, and application in supercapacitors. J Power Sources 246:621–628. doi:10.1016/j.jpowsour.2013.08.002

Frackowiak E (2007) Carbon materials for supercapacitor application. Phys Chem Chem Phys 9(15):1774–1785. doi:10.1039/b618139m

Frackowiak E, Béguin F (2001) Carbon materials for the electrochemical storage of energy in capacitors. Carbon 39(6):937–950. doi:10.1016/S0008-6223(00)00183-4

Frank S, Poncharal P, Wang ZL, Heer WAd (1998) Carbon nanotube quantum resistors. Science 280(5370):1744–1746. doi:10.1126/science.280.5370.1744

Fu Q, Gao B, Dou H, Hao L, Lu X, Sun K, Zhang X (2011) Novel non-covalent sulfonated multiwalled carbon nanotubes from p-toluenesulfonic acid/glucose doped polypyrrole for

electrochemical capacitors. Synth Met 161(5–6):373–378. doi:10.1016/j.synthmet.2010.12.009

Fu H, Du Z-J, Zou W, Li H-Q, Zhang C (2013) Carbon nanotube reinforced polypyrrole nanowire network as a high-performance supercapacitor electrode. J Mater Chem A 1(47):14943–14950. doi:10.1039/c3ta12844j

Gan JK, Lim YS, Pandikumar A, Huang NM, Lim HN (2015) Graphene/polypyrrole-coated carbon nanofiber core-shell architecture electrode for electrochemical capacitors. RSC Adv 5(17):12692–12699. doi:10.1039/c4ra14922j

Gupta VK, Kumar R, Nayak A, Saleh TA, Barakat MA (2013) Adsorptive removal of dyes from aqueous solution onto carbon nanotubes: a review. Adv Colloid Interface Sci 193–194:24–34. doi:10.1016/j.cis.2013.03.003

Han Y, Shen M, Lin X, Ding B, Zhang L, Tong H, Zhang X (2012) Ternary phase interfacial polymerization of polypyrrole/MWCNT nanocomposites with core-shell structure. Synth Met 162(9–10):753–758. doi:10.1016/j.synthmet.2012.03.001

Hussain S, Amade R, Jover E, Bertran E (2015) Growth and plasma functionalization of carbon nanotubes. J Clust Sci 26(2):315–336. doi:10.1007/s10876-015-0862-1

Izadi-Najafabadi A, Tan DTH, Madden JD (2005) Towards high power polypyrrole/carbon capacitors. Synth Met 152(1–3):129–132. doi:10.1016/j.synthmet.2005.07.094

Johnson DW, Dobson BP, Coleman KS (2015) A manufacturing perspective on graphene dispersions. Curr Opin Coll Interface Sci 20(5–6):367–382. doi:10.1016/j.cocis.2015.11.004

Jurewicz K, Delpeux S, Bertagna V, Béguin F, Frackowiak E (2001) Supercapacitors from nanotubes/polypyrrole composites. Chem Phys Lett 347(1–3):36–40. doi:10.1016/S0009-2614(01)01037-5

Kharisov BI, Kharissova OV, Leija Gutierrez H, Ortiz Méndez U (2009) Recent advances on the soluble carbon nanotubes. Ind Eng Chem Res 48(2):572–590. doi:10.1021/ie800694f

Khomenko V, Frackowiak E, Béguin F (2005) Determination of the specific capacitance of conducting polymer/nanotubes composite electrodes using different cell configurations. Electrochim Acta 50(12):2499–2506. doi:10.1016/j.electacta.2004.10.078

Kim P, Shi L, Majumdar A, McEuen PL (2001) Thermal transport measurements of individual multiwalled nanotubes. Phys Rev Lett 87(21):215502. doi:10.1103/PhysRevLett.87.215502

Kim J-Y, Kim KH, Kim KB (2008) Fabrication and electrochemical properties of carbon nanotube/polypyrrole composite film electrodes with controlled pore size. J Power Sources 176(1):396–402. doi:10.1016/j.jpowsour.2007.09.117

Kim BC, Hong J-Y, Wallace GG, Park HS (2015) Recent progress in flexible electrochemical capacitors: electrode materials, device configuration, and functions. Adv Energy Mat 5(22). doi:10.1002/aenm.201500959

Kuila T, Bose S, Mishra AK, Khanra P, Kim NH, Lee JH (2012) Chemical functionalization of graphene and its applications. Prog Mater Sci 57(7):1061–1105. doi:10.1016/j.pmatsci.2012.03.002

Kumar A, Singh RK, Singh HK, Srivastava P, Singh R (2014) Enhanced capacitance and stability of p-toluenesulfonate doped polypyrrole/carbon composite for electrode application in electrochemical capacitors. J Power Sources 246:800–807. doi:10.1016/j.jpowsour.2013.07.121

Lai L, Wang L, Yang H, Sahoo NG, Tam QX, Liu J, Lin J (2012) Tuning graphene surface chemistry to prepare graphene/polypyrrole supercapacitors with improved performance. Nano Energy 1(5):723–731. doi:10.1016/j.nanoen.2012.05.012

Lee H, Kim H, Cho MS, Choi J, Lee Y (2011) Fabrication of polypyrrole (PPy)/carbon nanotube (CNT) composite electrode on ceramic fabric for supercapacitor applications. Electrochim Acta 56(22):7460–7466. doi:10.1016/j.electacta.2011.06.113

Li X, Zhitomirsky I (2013) Electrodeposition of polypyrrole-carbon nanotube composites for electrochemical supercapacitors. J Power Sources 221:49–56. doi:10.1016/j.jpowsour.2012.08.017

Li J, Zhan H, Zhou Y (2003) Synthesis and electrochemical properties of polypyrrole-coated poly(2,5-dimercapto-1,3,4-thiadiazole). Electrochem Commun 5(7):555–560. doi:10.1016/S1388-2481(03)00121-8

Li D, Muller MB, Gilje S, Kaner RB, Wallace GG (2008) Processable aqueous dispersions of graphene nanosheets. Nat Nanotechnol 3(2):101–105. doi:10.1038/nnano.2007.451

Li X, Imin P, Adronov A, Zhitomirsky I (2012) Effect of 5-sulfosalicylic acid and poly 2,5-bis(3-sulfonatopropoxy)-1,4-ethynylphenylene-alt-1,4-ethynylphenylene on electrodeposition of polypyrrole-carbon nanotube films on stainless steel. Mater Lett 68:24–27. doi:10.1016/j.matlet.2011.10.010

Li J, Xie H, Li Y (2013) Fabrication of graphene oxide/polypyrrole nanowire composite for high performance supercapacitor electrodes. J Power Sources 241:388–395. doi:10.1016/j.jpowsour.2013.04.144

Li P, Shi E, Yang Y, Shang Y, Peng Q, Wu S, Wu D (2014) Carbon nanotube-polypyrrole core-shell sponge and its application as highly compressible supercapacitor electrode. Nano Res 7(2):209–218. doi:10.1007/s12274-013-0388-5

Liang K, Gu T, Cao Z, Tang X, Hu W, Wei B (2014) In situ synthesis of SWNTs@MnO$_2$/polypyrrole hybrid film as binder-free supercapacitor electrode. Nano Energy 9:245–251. doi:10.1016/j.nanoen.2014.07.017

Lim YS, Lim HN, Lim SP, Huang NM (2014) Catalyst-assisted electrochemical deposition of graphene decorated polypyrrole nanoparticles film for high-performance supercapacitor. RSC Adv 4(99):56445–56454. doi:10.1039/c4ra09234a

Lin XQ, Xu YH (2008) Facile synthesis and electrochemical capacitance of composites of polypyrrole/multi-walled carbon nanotubes. Electrochim Acta 53(15):4990–4997. doi:10.1016/j.electacta.2008.02.020

Liu C, Li F, Ma LP, Cheng HM (2010) Advanced materials for Energy Storage. Adv Mater, 22(8) E28-+. doi: 10.1002/adma.200903328

Liu J, An J, Ma Y, Li M, Ma R (2012) Synthesis of a graphene-polypyrrole nanotube composite and its application in supercapacitor electrode. J Electrochem Soc 159(6):A828–A833. doi:10.1149/2.093206jes

Liu F, Han G, Chang Y, Fu D, Li Y, Li M (2014) Fabrication of carbon nanotubes/polypyrrole/carbon nanotubes/melamine foam for supercapacitor. J App Poly Sci 131(2):39779. doi:10.1002/app.39779

Liu X, Qian T, Xu N, Zhou J, Guo J, Yan C (2015) Preparation of on chip, flexible supercapacitor with high performance based on electrophoretic deposition of reduced graphene oxide/polypyrrole composites. Carbon 92:348–353. doi:10.1016/j.carbon.2015.05.039

Lu X, Dou H, Yuan C, Yang S, Hao L, Zhang F, Zhang X (2012a) Polypyrrole/carbon nanotube nanocomposite enhanced the electrochemical capacitance of flexible graphene film for supercapacitors. J Power Sources 197:319–324. doi:10.1016/j.jpowsour.2011.08.112

Lu X, Zhang F, Dou H, Yuan C, Yang S, Hao L, Zhang X (2012b) Preparation and electrochemical capacitance of hierarchical graphene/polypyrrole/carbon nanotube ternary composites. Electrochim Acta 69:160–166. doi:10.1016/j.electacta.2012.02.107

Mao L, Chan HSO, Wu J (2012) Cetyltrimethylammonium bromide intercalated graphene/polypyrrole nanowire composites for high performance supercapacitor electrode. RSC Advances 2(28):10610–10617. doi:10.1039/c2ra21617e

Marchesi LFQP, Simoes FR, Pocrifka LA, Pereira EC (2011) Investigation of polypyrrole degradation using electrochemical impedance spectroscopy. J Phys Chem B 115(31):9570–9575. doi:10.1021/jp2041263

Meyyappan M (2013) Nanostructured materials for supercapacitors. J Vac Sci Technol A 31(5):14. doi:10.1116/1.4802772

Mini PA, Balakrishnan A, Nair SV, Subramanian KRV (2011) Highly super capacitive electrodes made of graphene/poly(pyrrole). Chem Commun 47(20):5753–5755. doi:10.1039/c1cc00119a

Muthulakshmi B, Kalpana D, Pitchumani S, Renganathan NG (2006) Electrochemical deposition of polypyrrole for symmetric supercapacitors. J Power Sources 158(2):1533–1537. doi:10.1016/j.jpowsour.2005.10.013

NuLi Y, Guo Z, Liu H, Yang J (2007) A new class of cathode materials for rechargeable magnesium batteries: organosulfur compounds based on sulfur–sulfur bonds. Electrochem Commun 9(8):1913–1917. doi:10.1016/j.elecom.2007.05.009

Nyholm L, Nystrom G, Mihranyan A, Stromme M (2011) Toward flexible polymer and paper-based energy storage devices. Adv Mater 23(33):3751–3769. doi:10.1002/adma.201004134

Otero TF, Grande H-J, Rodríguez J (1997) Reinterpretation of polypyrrole electrochemistry after consideration of conformational relaxation processes. J Phys Chem B 101(19):3688–3697. doi:10.1021/jp9630277

Pandolfo AG, Hollenkamp AF (2006) Carbon properties and their role in supercapacitors. J Power Sources 157(1):11–27. doi:10.1016/j.jpowsour.2006.02.065

Paul S, Lee Y-S, Choi J-A, Kang YC, Kim D-W (2010) Synthesis and electrochemical characterization of polypyrrole/multi-walled carbon nanotube composite electrodes for supercapacitor applications. Bull Korean Chem Soc 31(5):1228–1232. doi:10.5012/bkcs.2010.31.5.1228

Paul S, Choi KS, Lee DJ, Sudhagar P, Kang YS (2012) Factors affecting the performance of supercapacitors assembled with polypyrrole/multi-walled carbon nanotube composite electrodes. Electrochim Acta 78:649–655. doi:10.1016/j.electacta.2012.06.088

Pei S, Cheng H-M (2012) The reduction of graphene oxide. Carbon 50(9):3210–3228. doi:10.1016/j.carbon.2011.11.010

Peng B, Locascio M, Zapol P, Li S, Mielke SL, Schatz GC, Espinosa HD (2008) Measurements of near-ultimate strength for multi-walled carbon nanotubes and irradiation-induced crosslinking improvements. Nat Nanotechnol 3(10):626–631. doi:10.1038/nnano.2008.211

Peng Y-J, Wu T-H, Hsu C-T, Li S-M, Chen M-G, Hu C-C (2014) Electrochemical characteristics of the reduced graphene oxide/carbon nanotube/polypyrrole composites for aqueous asymmetric supercapacitors. J Power Sources 272:970–978. doi:10.1016/j.jpowsour.2014.09.022

Qi K, Qiu Y, Guo X (2014) Pulse electrochemical incorporation of graphene oxide into polypyrrole films for supercapacitor electrode materials. Electrochim Acta 137:685–692. doi:10.1016/j.electacta.2014.06.083

Raj CJ, Kim BC, Cho W-J, Lee W-G, Jung S-D, Kim YH, Yu KH (2015) Highly flexible and planar supercapacitors using graphite flakes/polypyrrole in polymer lapping film. ACS appl mater interfaces 7(24):13405–13414. doi:10.1021/acsami.5b02070

Raudsepp T, Marandi M, Tamm T, Sammelselg V, Tamm J (2008) Study of the factors determining the mobility of ions in the polypyrrole films doped with aromatic sulfonate anions. Electrochim Acta 53(11):3828–3835. doi:10.1016/j.electacta.2007.11.059

Raymundo-Pinero E, Cadek M, Wachtler M, Beguin F (2011) Carbon nanotubes as nanotexturing agents for high power supercapacitors based on seaweed carbons. Chemsuschem 4(7):943–949. doi:10.1002/cssc.201000376

Sadki S, Schottland P, Brodie N, Sabouraud G (2000) The mechanisms of pyrrole electropolymerization. Chem Soc Rev 29(5):283–293. doi:10.1039/A807124A

Sharma RK, Rastogi AC, Desu SB (2008) Pulse polymerized polypyrrole electrodes for high energy density electrochemical supercapacitor. Electrochem Commun 10(2):268–272. doi:10.1016/j.elecom.2007.12.004

Shi C, Zhitomirsky I (2011) Electrodeposition of composite polypyrrole-carbon nanotube films. Surf Eng 27(9):655–661. doi:10.1179/1743294410y.0000000004

Shi K, Zhitomirsky I (2013a) Electrophoretic nanotechnology of graphene-carbon nanotube and graphene-polypyrrole nanofiber composites for electrochemical supercapacitors. J Colloid Interface Sci 407:474–481. doi:10.1016/j.jcis.2013.06.058

Shi K, Zhitomirsky I (2013b) Fabrication of polypyrrole-coated carbon nanotubes using oxidant-surfactant nanocrystals for supercapacitor electrodes with high mass loading and enhanced performance. ACS App Mater Interfaces 5(24):13161–13170. doi:10.1021/am404159b

Shi K, Zhitomirsky I (2013c) Polypyrrole nanofiber-carbon nanotube electrodes for supercapacitors with high mass loading obtained using an organic dye as a co-dispersant. J Mater Chem A 1(38):11614–11622. doi:10.1039/c3ta12466e

Shi K, Zhitomirsky I (2015a) Asymmetric supercapacitors based on activated-carbon-coated carbon nanotubes. Chemelectrochem 2(3):396–403. doi:10.1002/celc.201402343

Shi K, Zhitomirsky I (2015b) Influence of chemical structure of dyes on capacitive dye removal from solutions. Electrochim Acta 174:588–595. doi:10.1016/j.electacta.2015.06.029

Shi K, Ren M, Zhitomirsky I (2014) Activated carbon-coated carbon nanotubes for energy storage in supercapacitors and capacitive water purification. Acs Sustain Chem Eng 2(5):1289–1298. doi:10.1021/sc500118r

Shi K, Pang X, and Zhitomirsky I (2015) Fabrication of Tiron-doped polypyrrole/MWCNT composite electrodes with high mass loading and enhanced performance for supercapacitors. J App Polymer Sci 132(32). doi:10.1002/app.42376

Simon P, Gogotsi Y (2008) Materials for electrochemical capacitors. Nat Mater 7(11):845–854. doi:10.1038/nmat2297

Singh A, Chandra A (2013) Graphite oxide/polypyrrole composite electrodes for achieving high energy density supercapacitors. J Appl Electrochem 43(8):773–782. doi:10.1007/s10800-013-0573-y

Snook GA, Kao P, Best AS (2011) Conducting-polymer-based supercapacitor devices and electrodes. J Power Sources 196(1):1–12. doi:10.1016/j.jpowsour.2010.06.084

Su Y, Zhitomirsky I (2015) Asymmetric electrochemical supercapacitor, based on polypyrrole coated carbon nanotube electrodes. Appl Energy 153:48–55. doi:10.1016/j.apenergy.2014.12.010

Sun X, Xu Y, Wang J (2012) Electropolymerized composite film of polypyrrole and functionalized multi-walled carbon nanotubes: effect of functionalization time on capacitive performance. J Solid State Electrochem 16(5):1781–1789. doi:10.1007/s10008-011-1619-x

Syritski V, Öpik A, Forsén O (2003) Ion transport investigations of polypyrroles doped with different anions by EQCM and CER techniques. Electrochim Acta 48(10):1409–1417. doi:10.1016/S0013-4686(03)00018-5

Tao J, Liu N, Ma W, Ding L, Li L, Su J, Gao Y (2013) Solid-state high performance flexible supercapacitors based on polypyrrole-MnO$_2$-carbon fiber hybrid structure. Sci Reports 3. doi:10.1038/srep02286

Tasis D, Tagmatarchis N, Bianco A, Prato M (2006) Chemistry of carbon nanotubes. Chem Rev 106(3):1105–1136. doi:10.1021/cr050569o

Treacy MMJ, Ebbesen TW, Gibson JM (1996) Exceptionally high Young's modulus observed for individual carbon nanotubes. Nature 381(6584):678–680. doi:10.1038/381678a0

Wang H (2009) Dispersing carbon nanotubes using surfactants. Curr Opin Colloid Interface Sci 14(5):364–371. doi:10.1016/j.cocis.2009.06.004

Wang JP, Zhang DH (2013) One-dimensional nanostructured polyaniline: syntheses, morphology controlling, formation mechanisms, new features, and applications. Adv Polym Technol 32:E323–E368. doi:10.1002/adv.21283

Wang J, Xu Y, Chen X, Sun X (2007) Capacitance properties of single wall carbon nanotube/polypyrrole composite films. Compos Sci Technol 67(14):2981–2985. doi:10.1016/j.compscitech.2007.05.015

Wang Y, Shi Z, Huang Y, Ma Y, Wang C, Chen M, Chen Y (2009) Supercapacitor devices based on graphene materials. J Phy Chem C 113(30):13103–13107. doi:10.1021/jp902214f

Wang JP, Xu YL, Wang J, Du XF, Xiao F, Li JB (2010) High charge/discharge rate polypyrrole films prepared by pulse current polymerization. Synth Met 160(17–18):1826–1831. doi:10.1016/j.synthmet.2010.06.020

Wang J, Xu Y, Wang J, Du X (2011) Toward a high specific power and high stability polypyrrole supercapacitors. Synth Met 161(11–12):1141–1144. doi:10.1016/j.synthmet.2011.01.011

Wang GP, Zhang L, Zhang JJ (2012a) A review of electrode materials for electrochemical supercapacitors. Chem Soc Rev 41(2):797–828. doi:10.1039/c1cs15060j

Wang J, Xu Y, Zhu J, Ren P (2012b) Electrochemical in situ polymerization of reduced graphene oxide/polypyrrole composite with high power density. J Power Sources 208:138–143. doi:10.1016/j.jpowsour.2012.02.018

Wang X, Yang C, Li H, Liu P (2013) Synthesis and electrochemical performance of well-defined flake-shaped sulfonated graphene/polypyrrole composites via facile in situ doping polymerization. Electrochim Acta 111:729–737. doi:10.1016/j.electacta.2013.08.145

Wang J, Xu Y, Wang J, Zhu J, Bai Y, Xiong L (2014a) Study on capacitance evolving mechanism of polypyrrole during prolonged cycling. J Phy Chem B 118(5):1353–1362. doi:10.1021/jp4054428

Wang JP, Tao XM, Li L (2014b) Study on horn-shaped polypyrrole prepared by pulse potential. Synth Met 194:176–181. doi:10.1016/j.synthmet.2014.04.026

Warren R, Sammoura F, Teh KS, Kozinda A, Zang X, Lin L (2015) Electrochemically synthesized and vertically aligned carbon nanotube-polypyrrole nanolayers for high energy storage devices. Sens Actuators A-Phys 231:65–73. doi:10.1016/j.sna.2014.07.010

Weidlich C, Mangold KM, Jüttner K (2005) EQCM study of the ion exchange behaviour of polypyrrole with different counterions in different electrolytes. Electrochim Acta 50(7–8):1547–1552. doi:10.1016/j.electacta.2004.10.032

White RJ, Brun N, Budarin VL, Clark JH, Titirici MM (2014) Always look on the "light" side of life: sustainable carbon aerogels. Chemsuschem 7(3):670–689. doi:10.1002/cssc.201300961

Winter M, Brodd RJ (2004) What are batteries, fuel cells, and supercapacitors? Chem Rev 104(10):4245–4270. doi:10.1021/cr020730k

Wu T-M, Lin S-H (2006) Characterization and electrical properties of polypyrrole/multiwalled carbon nanotube composites synthesized by in situ chemical oxidative polymerization. J Polym Sci Part B 44(10):1413–1418. doi:10.1002/polb.20809

Wu Z, Chen Z, Du X, Logan JM, Sippel J, Nikolou M, Rinzler AG (2004) Transparent, conductive carbon nanotube films. Science (New York) 305(5688):1273–1276. doi:10.1126/science.1101243

Wu Y, Guo C, Li N, Ji L, Li Y, Tu Y, Yang X (2014) Three-dimensional interconnected nanocarbon hybrid prepared by one-pot synthesis method with polypyrrole-based nanotube and

graphene and the application in high-performance capacitance. Electrochim Acta 146:386–394. doi:10.1016/j.electacta.2014.09.055

Xiao Q, Zhou X (2003) The study of multiwalled carbon nanotube deposited with conducting polymer for supercapacitor. Electrochim Acta 48(5):575–580. doi:10.1016/S0013-4686(02)00727-2

Xu S, Yang H, Wang K, Wang B, Xu Q (2014) Effect of supercritical CO_2 on fabrication of free-standing hierarchical graphene oxide/carbon nanofiber/polypyrrole film and its electrochemical property. Phys Chem Chem Phys 16(16):7350–7357. doi:10.1039/c3cp54957g

Xu R, Guo F, Cui X, Zhang L, Wang K, Wei J (2015a) High performance carbon nanotube based fiber-shaped supercapacitors using redox additives of polypyrrole and hydroquinone. J Mater Chem A 3(44):22353–22360. doi:10.1039/c5ta06165b

Xu R, Wei J, Guo F, Cui X, Zhang T, Zhu H, Wu D (2015b) Highly conductive, twistable and bendable polypyrrole-carbon nanotube fiber for efficient supercapacitor electrodes. RSC Adv 5(28):22015–22021. doi:10.1039/c5ra01917f

Yang C, Liu P, Wang T (2011) Well-Defined core–shell carbon black/polypyrrole nanocomposites for electrochemical energy storage. ACS Appl Mater Interfaces 3(4):1109–1114. doi:10.1021/am1012529

Yang C, Shen J, Wang C, Fei H, Bao H, Wang G (2014) All-solid-state asymmetric supercapacitor based on reduced graphene oxide/carbon nanotube and carbon fiber paper/polypyrrole electrodes. J Mater Chem A 2(5):1458–1464. doi:10.1039/c3ta13953k

Yang L, Shi Z, Yang W (2015a) Polypyrrole directly bonded to air-plasma activated carbon nanotube as electrode materials for high-performance supercapacitor. Electrochim Acta 153:76–82. doi:10.1016/j.electacta.2014.11.146

Yang X, Liu A, Zhao Y, Lu H, Zhang Y, Wei W, Liu S (2015b) Three-dimensional macroporous polypyrrole-derived graphene electrode prepared by the hydrogen bubble dynamic template for supercapacitors and metal-free catalysts. ACS App Mater Interfaces 7(42):23731–23740. doi:10.1021/acsami.5b07982

Yang X, Shi K, Zhitomirsky I, Cranston ED (2015c) Cellulose nanocrystal aerogels as universal 3D lightweight substrates for supercapacitor materials. Adv Mater 27(40):6104–6109. doi:10.1002/adma.201502284

Ye S, Feng J (2014) Self-assembled three-dimensional hierarchical graphene/polypyrrole nanotube hybrid aerogel and its application for supercapacitors. ACS App Mater Interfaces 6(12):9671–9679. doi:10.1021/am502077p

Yu C, Ma P, Zhou X, Wang A, Qian T, Wu S, Chen Q (2014) All-solid-state flexible supercapacitors based on highly dispersed polypyrrole nanowire and reduced graphene oxide composites. ACS app mater interfaces 6(20):17937–17943. doi:10.1021/am5059603

Zhang J, Zhao XS (2012) Conducting polymers directly coated on reduced graphene oxide sheets as high-performance supercapacitor electrodes. J Phys Chem C 116(9):5420–5426. doi:10.1021/jp211474e

Zhang LL, Zhao S, Tian XN, Zhao XS (2010) Layered graphene oxide nanostructures with sandwiched conducting polymers as supercapacitor electrodes. Langmuir 26(22):17624–17628. doi:10.1021/la103413s

Zhang K, Mao L, Zhang LL, On Chan HS, Zhao XS, Wu J (2011) Surfactant-intercalated, chemically reduced graphene oxide for high performance supercapacitor electrodes. J Mater Chem 21(20):7302–7307. doi:10.1039/C1JM00007A

Zhang D, Dong Q-Q, Wang X, Yan W, Deng W, Shi L-Y (2013) Preparation of a three-dimensional ordered macroporous carbon nanotube/polypyrrole composite for supercapacitors and

diffusion modeling. J Phys Chem C 117(40):20446–20455. doi:10.1021/jp405850w

Zhang Y, Li M, Yang L, Yi K, Li Z, Yao J (2014) Facilely prepared polypyrrole-graphene oxide-sodium dodecylbenzene sulfonate nanocomposites by in situ emulsion polymerization for high-performance supercapacitor electrodes. J Solid State Electrochem 18(8):2139–2147. doi:10.1007/s10008-014-2469-0

Zhang Y, Zhen Z, Zhang Z, Lao J, Wei J, Wang K, Zhu H (2015) In-situ synthesis of carbon nanotube/graphene composite sponge and its application as compressible supercapacitor electrode. Electrochim Acta 157:134–141. doi:10.1016/j.electacta.2015.01.084

Zhao Y, Liu J, Hu Y, Cheng H, Hu C, Jiang C, Qu L (2013) Highly compression-tolerant supercapacitor based on polypyrrole-mediated graphene foam electrodes. Adv Mater 25(4):591–595. doi:10.1002/adma.201203578

Zhou X, Peng C, Chen GZ (2012) 20 V stack of aqueous supercapacitors with carbon (−), titanium bipolar plates and CNT-polypyrrole composite (+). Aiche J 58(3):974–983. doi:10.1002/aic.12632

Zhu Y, Zhitomirsky I (2013) Influence of dopant structure and charge on supercapacitive behavior of polypyrrole electrodes with high mass loading. Synth Met 185–186:126–132. doi:10.1016/j.synthmet.2013.10.015

Zhu Y, Murali S, Cai W, Li X, Suk JW, Potts JR, Ruoff RS (2010) Graphene and graphene oxide: synthesis, properties, and applications. Adv Mater 22(35):3906–3924. doi:10.1002/adma.201001068

Zhu C, Zhai J, Wen D, Dong S (2012) Graphene oxide/polypyrrole nanocomposites: one-step electrochemical doping, coating and synergistic effect for energy storage. J Mater Chem 22(13):6300–6306. doi:10.1039/c2jm16699b

Zhu Y, Shi K, Zhitomirsky I (2014a) Anionic dopant-dispersants for synthesis of polypyrrole coated carbon nanotubes and fabrication of supercapacitor electrodes with high active mass loading. J Mater Chem A 2(35):14666–14673. doi:10.1039/c4ta02117g

Zhu Y, Shi K, Zhitomirsky I (2014b) Polypyrrole coated carbon nanotubes for supercapacitor devices with enhanced electrochemical performance. J Power Sources 268:233–239. doi:10.1016/j.jpowsour.2014.06.046